Cell

Sneezing reflex is mediated by a peptidergic pathway from nose to brainstem

Graphical abstract

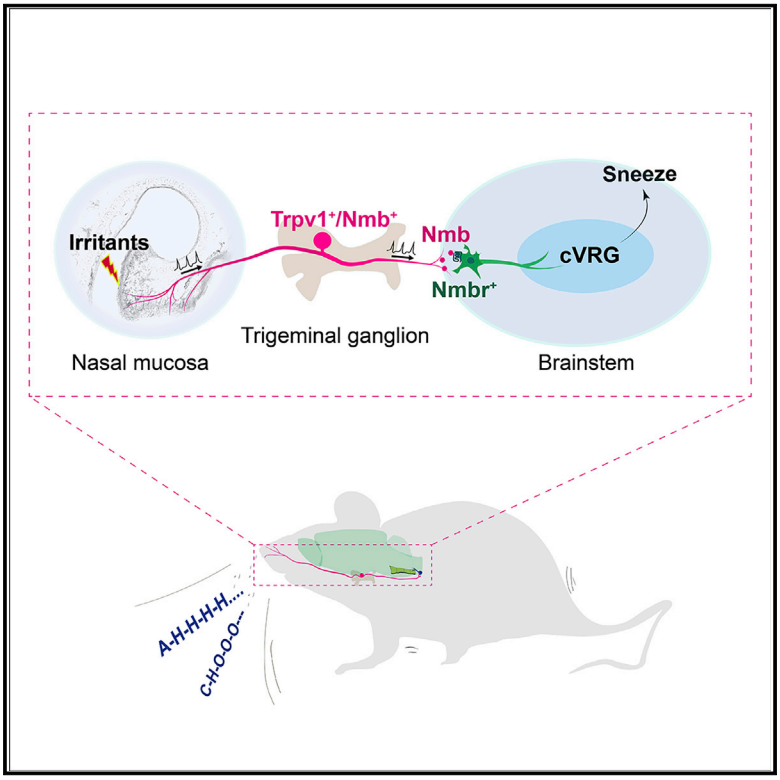

Authors

Fengxian Li, Haowu Jiang, Xiaolei Shen, ..., Zhoufeng Chen, Andrew J.W. Huang, Qin Liu

Correspondence

qinliu@wustl.edu

In brief

Using a newly developed mouse model, Li et al. elucidate the peptidergic pathway that mediates the sneezing reflex, offering insight into how sneezing occurs.

Highlights

- The first peptidergic pathway for chemically and allergy-induced sneezing
- Nasal sensory neurons release neuromedin B (NMB) to signal sneezing
- NMB activates central NMBR$^+$ neurons in the sneeze-evoking region of the brainstem
- NMBR$^+$ neurons synapse in the caudal ventral respiratory group to drive sneezing

Li et al., 2021, Cell *184*, 3762–3773
July 8, 2021
https://doi.org/10.1016/j.cell.2021.05.017

CellPress

CellPress

Cell

Article

Sneezing reflex is mediated by a peptidergic pathway from nose to brainstem

Fengxian Li,[1,8] Haowu Jiang,[1,8] Xiaolei Shen,[1] Weishan Yang,[1] Changxiong Guo,[1] Zhiyao Wang,[1] Maolei Xiao,[1] Lian Cui,[2] Wenqin Luo,[2] Brian S. Kim,[1,3] Zhoufeng Chen,[1,3,4,5] Andrew J.W. Huang,[6] and Qin Liu[1,3,6,7,9,*]

[1]Department of Anesthesiology, Center for the Study of Itch and Sensory Disorders, and Washington University Pain Center, Washington University School of Medicine, St. Louis, MO 63110, USA
[2]Department of Neuroscience, Perelman School of Medicine, University of Pennsylvania, Philadelphia, PA 19104, USA
[3]Division of Dermatology, Department of Medicine, Washington University School of Medicine, St. Louis, MO 63110, USA
[4]Department of Psychiatry, Washington University School of Medicine, St. Louis, MO 63110, USA
[5]Department of Developmental Biology, Washington University School of Medicine, St. Louis, MO 63110, USA
[6]Department of Ophthalmology & Visual Sciences, Washington University School of Medicine, St. Louis, MO 63110, USA
[7]Department of Neuroscience, Washington University School of Medicine, St. Louis, MO 63110, USA
[8]These authors contributed equally
[9]Lead contact
*Correspondence: qinliu@wustl.edu
https://doi.org/10.1016/j.cell.2021.05.017

SUMMARY

Sneezing is a vital respiratory reflex frequently associated with allergic rhinitis and viral respiratory infections. However, its neural circuit remains largely unknown. A sneeze-evoking region was discovered in both cat and human brainstems, corresponding anatomically to the central recipient zone of nasal sensory neurons. Therefore, we hypothesized that a neuronal population postsynaptic to nasal sensory neurons mediates sneezing in this region. By screening major presynaptic neurotransmitters/neuropeptides released by nasal sensory neurons, we found that neuromedin B (NMB) peptide is essential for signaling sneezing. Ablation of NMB-sensitive postsynaptic neurons in the sneeze-evoking region or deficiency in NMB receptor abolished the sneezing reflex. Remarkably, NMB-sensitive neurons further project to the caudal ventral respiratory group (cVRG). Chemical activation of NMB-sensitive neurons elicits action potentials in cVRG neurons and leads to sneezing behavior. Our study delineates a peptidergic pathway mediating sneezing, providing molecular insights into the sneezing reflex arc.

INTRODUCTION

Sneezing is a basic reflex that expels irritants and pathogens from the airway. Although designed to be a defense mechanism, sneezing is associated with many viral respiratory infections (e.g., common cold and flu) and allergic rhinitis (a.k.a., hay fever) and severely impacts our quality of life and productivity (Songu and Cingi, 2009). Moreover, sneezing represents the most forceful and common mechanism to spread infectious droplets during viral respiratory infections. Studies indicate that a single sneeze can create 40,000 virus-containing droplets that reach a radius of 7 to 8 m and suspend in the air for up to 10 min (Bourouiba, 2016, 2020; Bourouiba et al., 2014; Cole and Cook, 1998; Scharfman et al., 2016; Tang et al., 2006). In contrast, a cough produces 3,000 droplets at most, which is about the same number as talking continuously for 5 min (Cole and Cook, 1998; Tang et al., 2006). Hence, sneezing is an important mechanism behind the community spread of many respiratory viruses. From the perspective of either basic science or clinical medicine, it is of paramount importance to understand the mechanisms underlying sneezing.

A sneeze-evoking region was discovered in the ventromedial spinal trigeminal nucleus (SpV) of both cats and humans (Hersch, 2000; Nonaka et al., 1990; Seijo-Martínez et al., 2006). Electrical stimulations of this region evoke sneeze-like responses in cats (Nonaka et al., 1990). Stroke-induced lesions on this region lead to paroxysmal sneezing or loss of ability to sneeze in humans (Hersch, 2000; Seijo-Martínez et al., 2006). However, the lack of information on the molecular identities of the neurons mediating sneezing in this region and related synaptic pathway impedes further investigation.

The sneeze-evoking region corresponds anatomically to the central recipient zone of the ethmoidal nerve that provides sensory branches to the nasal mucosa (Hersch, 2000; Lucier and Egizii, 1986; Nonaka et al., 1990; Seijo-Martínez et al., 2006), suggesting that the region comprises the postsynaptic neurons of nasal sensory neurons. We therefore hypothesize that a specific population of postsynaptic neurons in the sneeze-evoking region mediates the sneezing reflex. Previous studies have shown that stimulation of nasal sensory fibers or ethmoidal nerve triggers sneezing in both cats and humans (Batsel and Lines, 1978; Geppetti et al., 1988; Hydén and Arlinger, 2007; Satoh

et al., 1998; Taylor-Clark et al., 2005; Wallois et al., 1991, 1997). However, it remains unclear which population of nasal sensory neurons initiates the sneezing reflex and which neurotransmitters/neuropeptides in nasal sensory neurons are required for transmitting sneeze signals. Lacking this information greatly impedes the study of the postsynaptic neurons in the sneeze-evoking region and hinders testing our hypothesis.

Sneezing is a reflex generated by central respiratory neurons. Nevertheless, the sneeze-evoking region is located within the ventromedial SpV and does not overlap with any reported respiratory centers in the brainstem (Feldman et al., 2013). It is therefore reasonable to speculate that the sneeze-evoking region further projects to central respiratory groups. Studies have characterized sneeze-related electrical activities in different groups of central respiratory neurons in cats (Batsel and Lines, 1978; Jakus et al., 1985; Orem and Brooks, 1986; Wallois et al., 1997). As sneezes interrupt the normal pattern of respiration, whether these electrical activities are the ''drivers'' or ''passengers'' of sneezing and whether they are induced by inputs from the sneeze-evoking region remain unknown.

In this study, we reveal the molecular identities of the neurons mediating sneezing in the sneeze-evoking region and delineate their anatomical and functional connections with central respiratory neurons. We developed a two-step reverse screening strategy to identify the neuronal population essential for sneezing in the sneeze-evoking region. First, we screened all major presynaptic neurotransmitters/neuropeptides released by nasal sensory neurons for sneeze signaling and identified the neuropeptide that is critically required for transmitting sneeze signals. Second, we targeted the corresponding postsynaptic neurons in the sneeze-evoking region, and studied their role in mediating sneezing. This strategy successfully helped us identify a highly restricted neuronal population that is key for the sneezing reflex in the sneeze-evoking region. To further determine which populations of respiratory neurons are the projection target(s) of the sneeze-evoking region, we conducted neuronal tracing, electrophysiology recording, and behavioral studies. These studies reveal that the caudal ventral respiratory group (cVRG) is a direct projection target of the sneeze-evoking region and drives the generation of sneezes. Collectively, we delineate the peptidergic pathway from nasal sensory neurons to central respiratory neurons that mediates the sneezing reflex. This newly defined pathway greatly advances our understanding of the neural mechanism underlying the sneezing reflex and has important implications in the development of therapeutic strategies for pathological sneezing.

RESULTS

Establishment of a sneezing model in mice

Sneezing is characterized by convulsive expulsion of air and the sound ''achoo'' in humans. However, most previous studies used anesthetized or decerebrate cats that could not make real sneezes and monitored fictive sneezing represented by diaphragmatic and intercostal muscle activities and related nerve activity (Batsel and Lines, 1978; Nonaka et al., 1990; Satoh et al., 1998; Wallois et al., 1991, 1997). To study the neural mechanism underlying the sneezing reflex, we established a behavioral model in freely moving mice. Studies have shown that capsaicin (a pungent compound from chili pepper) and histamine elicit sneezes in humans (Doyle et al., 1990; Geppetti et al., 1988; Tønnesen and Mygind, 1985). By delivering aerosolized droplets containing capsaicin or histamine via a nebulizer to the mouse test chambers, we found that both compounds triggered sneeze-like responses in mice (Figures 1A and 1B). Specifically, the audio recording revealed sneeze-like episodes characterized by audio peaks, which comprise both sonic and ultrasonic components and are distinct from nociception-associated vocalization (Figures 1A and S1; Video S1). Whole-body plethysmography (WBP) showed repetitive sneeze-like respiratory patterns characterized by forceful and convulsive expiration (Figure 1A). The respiratory patterns and audio peaks correlate well, as revealed by simultaneous WBP and audio recordings (Figure 1A; Table S1; Video S2). To confirm that the audio and respiratory responses are sneezes and not other respiratory reflexes, we examined whether these responses are mediated by sensory fibers innervating the nasal mucosa rather than those in the trachea, lung, or other sites. The anterior ethmoidal nerve (AEN) provides sensory branches to the nasal mucosa and plays an essential role in triggering sneezes (Batsel and Lines, 1978; Satoh et al., 1998; Wallois et al., 1991, 1997). After transecting AEN, we found that the audio- and respiratory responses to both capsaicin and histamine were significantly reduced compared with the sham surgery group (Figure 1B), confirming that these responses are sneezes mediated by nasal sensory fibers.

Convulsive expulsion of air and associated sound are generated by sudden and involuntary muscular movements during sneezing. By conducting electromyography (EMG) recording of the diaphragm and external oblique abdominus of lightly anesthetized mice, we observed sudden and involuntary muscular movements upon nasal challenge of capsaicin (Figure 1C), consistent with sneezing-related muscular movement in cats (Nonaka et al., 1990; Satoh et al., 1998). To confirm that the recorded muscular movements faithfully reflect sneezing in mice, we ablated nasal sensory fibers that express Trpv1, a capsaicin-sensitive cation channel. This ablation abolished capsaicin-induced muscular movements, as revealed by EMG (Figure 1D). These results confirm that the recorded muscular movements are triggered by nasal sensory fibers and faithfully reflect sneezing, but not other respiratory responses (e.g., coughing mediated by sensory fibers in the lower airway), in mice. In addition to muscular movement, nasal secretion is also significantly increased after capsaicin-induced sneezing (Figure 1E). Together, our studies firmly establish the mouse sneezing model.

Small-diameter sensory neurons mediate both chemically induced and allergy-associated sneezing

Sensory neurons are highly heterogeneous and can be grossly classified into two groups, myelinated large-diameter neurons that detect innocuous stimuli (e.g., light touch) and thinly myelinated or unmyelinated small-diameter neurons that detect noxious stimuli. To screen the presynaptic neurotransmitters/neuropeptides essential for sneeze signaling in an efficient and precise manner, we first sought to determine which group

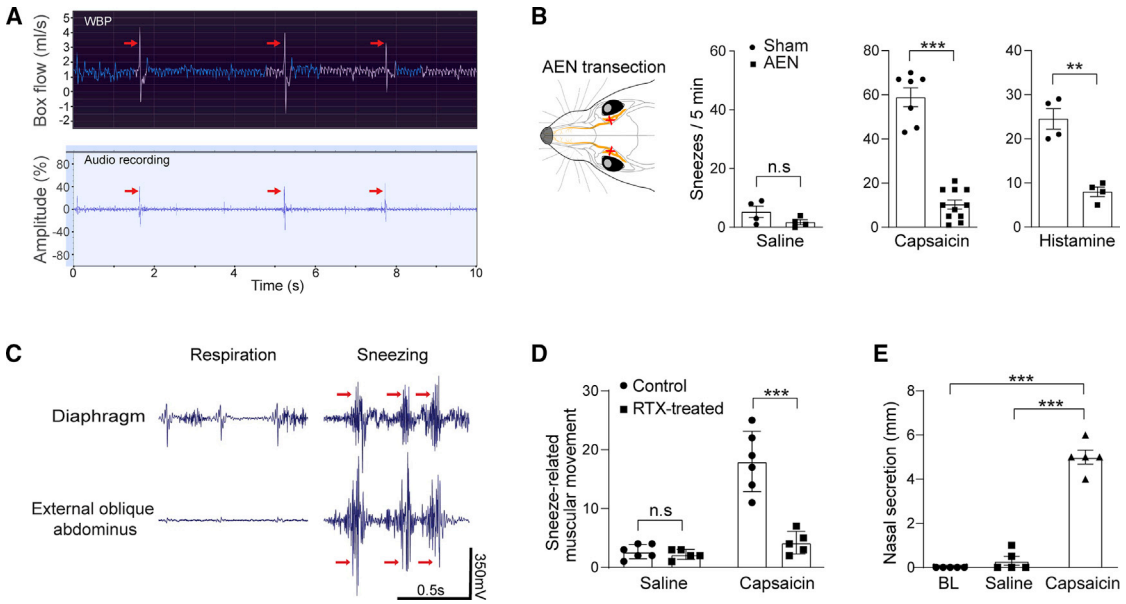

Figure 1. Establishing the mouse sneeze model

(A) Representative traces showing the simultaneous whole-body plethysmography (WBP) and audio recordings of a freely moving WT mouse upon exposure to aerosolized capsaicin solution (12 μM). The WBP and audio peaks (indicated by the arrows) correlate well and indicate sneezing-like responses.

(B) Transection of the anterior ethmoidal nerve (AEN), which provides sensory innervation to the nose, significantly reduced sneezing-like responses to aerosolized capsaicin (12 μM) and histamine (100 mM) solution.

(C) Electromyography (EMG) recording showing the representative muscle contractions of diaphragm and external oblique abdominus of mice in eupnea and during sneezing responses to nasal challenge of capsaicin (12 μM). Muscular contractions that significantly increase over regular respiratory movement and interrupt the respiratory rhythm were counted as sneezing-related responses (indicated by red arrows).

(D) Nasal instillation of resiniferatoxin (RTX; 50 ng in 2 μL/nostril) ablated nasal Trpv1$^+$ sensory fibers and eliminated sneezing-related muscular responses to capsaicin, as revealed by EMG recording.

(E) Nasal secretion was significantly increased after capsaicin-induced sneezes compared with baseline (BL) or saline control.

Each dot represents an individual mouse (n = 4–11 mice/group). Data are represented as mean ± SEM. **p ≤ 0.01; ***p ≤ 0.001; n.s, not significant. See also Figure S1, Videos S1 and S2, and Table S1.

of sensory neurons mediates sneezing. As sneezes can be readily elicited by capsaicin and histamine in humans and mice (see Figure 1) (Doyle et al., 1990; Geppetti et al., 1988; Tønnesen and Mygind, 1985), we examined the nasal innervation of sensory neurons that express Trpv1, the capsaicin-sensitive cation channel that also serves as the downstream transduction channel of histamine H1r receptor (Caterina et al., 1997; Shim et al., 2007). Trpv1 is expressed by many thinly myelinated or unmyelinated small-diameter neurons. Utilizing *Trpv1*$^{PLAP/+}$ reporter line (Cavanaugh et al., 2011), we found that Trpv1$^+$ sensory fibers richly innervate the nasal mucosa and comprise a major population of nasal sensory fibers (Figures 2A and 2B).

To study the role of Trpv1$^+$ small-diameter neurons in triggering sneezes, we instilled a small volume (2 μL) of resiniferatoxin (RTX) solution into the mouse nasal cavity to ablate Trpv1$^+$ nasal sensory fibers (Figure 2C) (Karai et al., 2004). After RTX treatment, audio and respiratory recordings revealed a significant reduction in the sneezing responses to capsaicin and histamine (Figures 2D and 2E). Furthermore, allergy-associated sneezing was also significantly reduced by desensitization of Trpv1$^+$ nasal afferent fibers (Figure 2F). These results reveal the central role of Trpv1$^+$ small-diameter neurons in mediating sneezing induced by both chemical irritants and allergens.

Neuromedin B is required for signaling sneezing

The identification of Trpv1$^+$ nasal small-diameter sensory neurons in eliciting sneezing allows for targeted screening of neurotransmitters/neuropeptides essential for signaling sneezing. First, we investigated which neurotransmitters and neuropeptides are expressed in Trpv1$^+$ nasal small-diameter neurons. Among all major neurotransmitters/neuropeptides identified in primary sensory neurons, Trpv1$^+$ nasal sensory neurons selectively express vesicular glutamate transporter 2 (*Vglut2*), neuropeptides substance P (*Tac1*), CGRP (*Calca*), and neuromedin B (NMB; *Nmb*) as revealed by single-cell RT-PCR (Figure 3A). Second, we studied which neurotransmitters/neuropeptides are required for transmitting sneeze signals by examining the sneezing responses of mice deficient in each neurotransmitter or neuropeptide. *Trpv1*$^{Cre/+}$;*Vglut2*$^{F/F}$ conditional knockout mice failed to show a significant reduction in their sneezing responses to capsaicin compared with control littermates (Figure 3B), indicating that Vglut2-dependent glutamate signaling is dispensable for signaling sneezing. Furthermore, deficiency in the neuropeptide substance P or CGRP did not affect the sneezing responses either (Figures 3C and 3D).

Interestingly, deficiency in the neuropeptide NMB significantly reduced the sneezing responses to capsaicin (Figure 3E), without altering other respiratory parameters examined (Figure S2). NMB

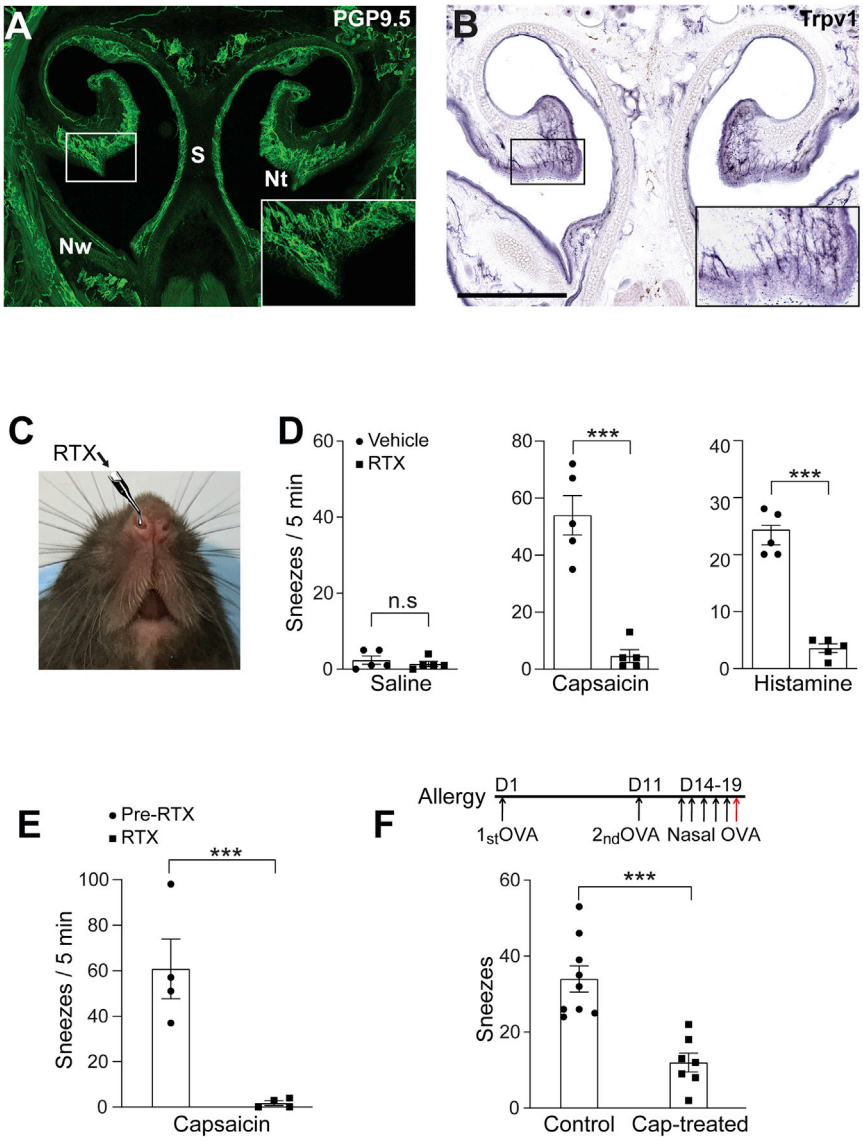

Figure 2. Trpv1-expressing nasal sensory fibers mediate both chemically induced and allergy-associated sneezing

(A) The mouse nose is densely innervated by primary sensory fibers (green), as revealed by immunostaining for PGP9.5, a pan-neuronal marker. The inset shows a higher-magnification view of the boxed area. Nt, nasal turbinate; S, nasal septum; Nw, nasal wall.

(B) Histochemistry for placental alkaline phosphatase (PLAP) revealed that Trpv1-expressing sensory fibers densely innervate the nasal mucosal membrane lining the nasal turbinate and septum in *Trpv1*$^{PLAP/+}$ transgenic mice. The inset shows a higher-magnification view of the boxed area.

(C) Nasal instillation of resiniferatoxin (RTX, 50 ng in 2 μL/nostril) to desensitize/degenerate Trpv1-expressing sensory fibers in the nose.

(D and E) Nasal instillation of RTX eliminated sneezing responses to aerosolized capsaicin (12 μM) and histamine (100 mM) solution, as revealed by (D) audio and (E) WBP recordings.

(F) Generation of allergic rhinitis mouse model. The red arrow indicates the intranasal instillation of allergen (ovalbumin [OVA]; 0.2 μg in 2 μL PBS/nostril) for sneezing test after two systemic immunizations and 5 days of nasal sensitization. Allergen-induced sneezing response was significantly reduced in capsaicin-pretreated mice compared with vehicle-treated control mice.

All images shown are representatives of three biologically independent mice. Scale bar, 500 μm. Each dot represents an individual mouse (n = 4–9 mice/group). Data are represented as mean ± SEM. ***p ≤ 0.001; n.s, not significant.

deficiency also resulted in an abolishment of sneezing responses to histamine (Figure 3E), one of principal mast cell mediators in allergic rhinitis (Uzzaman and Story, 2012). In addition to histamine, mast cells release many other mediators, including serotonin and various neuropeptides (Kushnir-Sukhov et al., 2007; Lee et al., 2008). However, the role of histamine-independent pathways in mediating sneezing remains poorly defined. We found that serotonin induces significant sneezing in mice (Figure 3F), correlating well with studies showing that serotonin induces sneezing in humans (Tønnesen and Mygind, 1985). Importantly, this sneezing response was abolished in *Nmb*-deficient mice (Figure 3F). Besides serotonin, neuropeptide FF (NPFF) is released from mast cells upon degranulation as shown by our previous study (Lee et al., 2008). Although NPFF has never been implicated in allergic sneezing, we found that NPFF induces significant sneezing responses in wild-type (WT) mice, but not *Nmb*$^{-/-}$ mice (Figure 3G). These results reveal the essential role of NMB peptide in signaling both histamine-dependent and independent sneezing responses and suggest its involvement in allergic sneezing. Further study indeed showed that NMB deficiency resulted in an abolishment of sneezing responses to mast-cell-dependent allergy (Figures 3H and 3I). Together, these results demonstrate that NMB is critically required for signaling sneezing.

As nasal challenge of capsaicin evokes sneezes and burning pain in humans (Geppetti et al., 1988), we next investigated whether there is any dose-dependent effect of capsaicin in inducing sneezes and pain and whether NMB is required for signaling pain. Interestingly, we found an inverse dose-response relationship between capsaicin doses and sneezing responses in WT mice. High-dose capsaicin induced fewer sneezes than low-dose capsaicin (Figure 3J). In contrast, pain-related behavior is evoked by capsaicin in a positive dose-dependent manner. While high-dose capsaicin induced fewer sneezes, it evoked more nose wiping (stereotypic behavior indicative of pain; Figure 3K) and more apnea episodes to reduce capsaicin inhalation (avoidance behavior; Figure 3L), revealing an antagonism between pain and sneezing. Interestingly, NMB deficiency

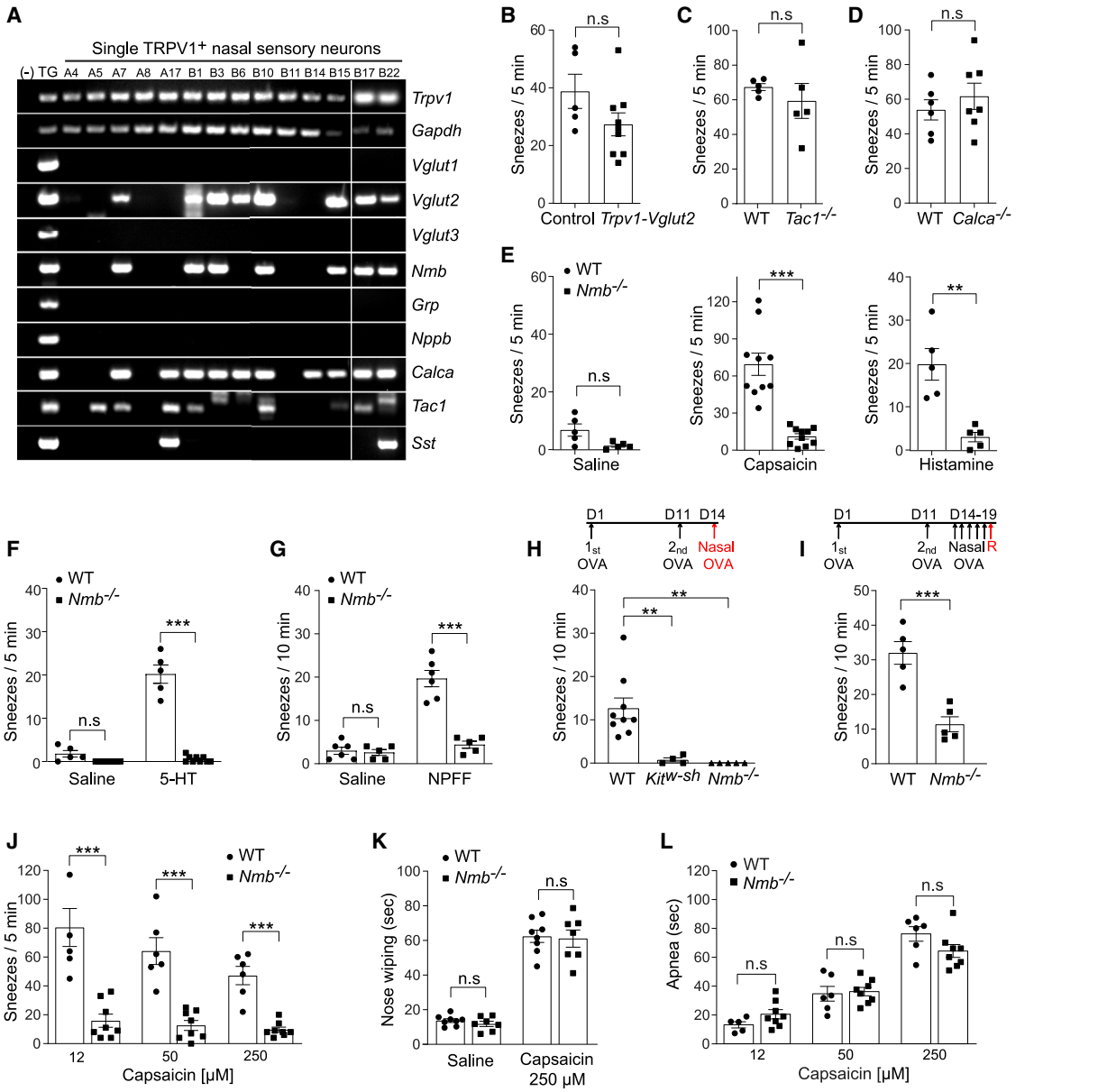

Figure 3. Neuromedin B is required for signaling sneezing

(A) Single-cell RT-PCR was performed on individual Trpv1$^+$ nasal sensory neurons that were labeled by intranasal application of fluorescent retrograde axonal tracer. Vesicular glutamate transporter 2 (*Vglut2*) and neuropeptides NMB (*Nmb*), CGRP (*Calca*), and substance P (*Tac1*) are selectively expressed by a majority of Trpv1$^+$ nasal neurons. In contrast, vesicular glutamate transporter 1 and 3 (*Vglut1* and *Vglut3*), gastrin-releasing peptide (*Grp*), natriuretic peptide B (*Nppb*), and somatostatin (*Sst*) are expressed by few or no Trpv1$^+$ nasal neurons. Whole trigeminal ganglia (TG) were used as a positive control. Genomic DNA served as a negative control (–) for intron-spanning primers used for RT-PCR.

(B–D) Deficiency in VGLUT2 (*Vglut2*), substance P (*Tac1*), or CGRP (*Calca*) does not affect the sneezing response to aerosolized capsaicin solution (12 μM) compared with control mice.

(E) Deficiency in the neuropeptide NMB (*Nmb*) abolishes the sneezing responses to aerosolized capsaicin (12 μM) and histamine (100 mM) solution.

(F and G) *Nmb* deficiency abolishes the sneezing responses to serotonin (5-HT; aerosolized solution [1 mM]) (F) and neuropeptide FF solution (NPFF; 20 nmol in 2 μL) (G).

(H) In an acute allergic model, the sneezing responses to allergen (OVA 0.2 μg in 2 μL PBS/nostril) were abolished in mast-cell-deficient *Kit*$^{w\text{-}sh}$ mice compared with WT controls. This mast-cell-dependent allergic sneezing was eliminated in *Nmb*$^{-/-}$ mice.

(I) *Nmb*$^{-/-}$ mice display reduced sneezing response in chronic allergic model compared with WT controls. The red arrow indicates the intranasal instillation of allergen (OVA 0.2 μg in 2 μL PBS/nostril) for sneezing test after 5 days of intranasal sensitization.

(J) Inverse dose-response relationship between capsaicin and sneezing responses in WT mice. *Nmb*$^{-/-}$ mice display reduced sneezing responses to capsaicin at all the doses tested.

(legend continued on next page)

abolished sneezing responses to capsaicin at both low and high doses tested (Figure 3J) but did not reduce pain-related nose wiping behavior or apnea induced by capsaicin (Figures 3K and 3L). These results indicate that NMB selectively signals sneezing, but not nasal pain-related behavior.

NMB is released from sensory neurons for signaling sneezing

Although NMB is highly expressed in trigeminal ganglia (TG), it is also detected in several brain regions, including the retrotrapezoid nucleus/parafacial respiratory group (RTN/pFRG) (Li et al., 2016; Wada et al., 1990). To determine whether NMB is released from primary sensory neurons to mediate sneezing, we first stimulated TG neurons with the sneeze-inducing chemicals histamine and capsaicin and found that both compounds elicited significant NMB release from TG neurons (Figures 4A and 4B). We then performed microinjection of NMB-specific small interfering RNA (siRNA) into the V1 division of TG, where most nasal sensory neurons are located (Figure 4C). The knockdown of *Nmb* in TG significantly reduced sneezing responses compared with pre-treatments and scrambled siRNA controls (Figures 4D and S3), indicating that NMB in sensory neurons is required for transmitting sneeze signals. In contrast, siRNA knockdown of *Nmb* in RTN did not affect sneezing responses (Figure 4E), suggesting that NMB plays distinct roles in the nasal sensory neurons and central RTN. To confirm the site of NMB action in signaling sneezing, we also generated $Trpv1^{Cre/+}$; $Nmb^{flox/flox}$ mice in which *Nmb* was conditionally knocked out in Trpv1-lineage sensory neurons (Figure 4F). $Trpv1^{Cre/+}$; $Nmb^{flox/flox}$ mice displayed significant reductions in their sneezing responses to capsaicin, histamine, and allergens (Figure 4G). These results demonstrate that NMB is released from sensory neurons to signal sneezing.

NMB-sensitive postsynaptic neurons in the sneeze-evoking region mediate sneezing

The essential role of NMB in signaling sneezing suggests the involvement of NMB-sensitive postsynaptic neurons within the sneeze-evoking region (i.e., the central recipient zone of nasal sensory neurons; see the diagram in Figure 5A). Indeed, capsaicin-induced sneezes led to a significantly increased expression of c-Fos within the sneeze-evoking region of WT mice, but not *Nmb*-deficient mice (Figures 5B and 5C), suggesting NMB-dependent transmission to the sneeze-evoking region. We further examined the role of NMB-sensitive postsynaptic neurons in signaling sneezing. Studies have shown that NMB-saporin efficiently ablates NMB-sensitive neurons (Mishra et al., 2012; Wan et al., 2017). Microinjection of NMB-saporin into the sneeze-evoking region abolished the sneezing responses to capsaicin and histamine (Figure 5D), suggesting that NMB-sensitive postsynaptic neurons mediate sneezing.

NMB acts by binding to its high-affinity cell-surface G-protein-coupled receptor, NMB receptor (NMBR) (Wada et al., 1991). We further tested whether NMBR is required for signaling sneeze. NMBR-deficient mice displayed significantly reduced sneezing responses to chemical and allergen stimuli (Figures 5E and 5F). Importantly, after sneeze-evoking stimulations, the c-Fos signal was barely detectable in the sneeze-evoking region of $Nmbr^{-/-}$ mice (Figures 5G and 5H), confirming the indispensable role of NMB-NMBR interaction in transmitting the sneeze-related signal.

$NMBR^+$ neurons represent a highly restricted population in the sneeze-evoking region and project to the cVRG

Sneezing is a reflex generated by central respiratory neurons. However, the sneeze-evoking region does not overlap with any reported respiratory regions in the brainstem. Hence, we hypothesize that $NMBR^+$ neurons further project to the central respiratory groups. To identify the projection targets of $NMBR^+$ neurons, we conducted axonal tracing of $NMBR^+$ neurons utilizing $Nmbr^{eGFP}$ reporter line (Wan et al., 2017). $NMBR^+$ neurons account for 9.1% ± 0.92% of total neurons in the sneeze-evoking region and comprise a highly restricted population (Figure 6A). Strikingly, we found that NMBR-GFP^+ axons richly innervate the cVRG, but not other respiratory regions, including the rostral ventral respiratory group (rVRG), pre-Bötzinger complex, and Bötzinger complex (Figures 6B and S4). Immunostaining for the presynaptic markers synaptophysin-1 indicates that $NMBR^+$ axons synapse with neurons in cVRG (Figure 6C). To confirm that NMBR-GFP^+ axons in cVRG originate from $NMBR^+$ neurons in the sneeze-evoking region, but not other brain regions, we microinjected Alexa-Fluor-555-conjugated cholera toxin subunit B (CTB; neuronal tracer) into cVRG of $Nmbr^{eGFP}$ mice for retrograde axonal tracing. The CTB-labeled NMBR-GFP^+ neurons are localized within the sneeze-evoking region and absent from other brain regions, including the pre-Bötzinger complex and nucleus tractus solitarius (NTS) (Figures 6D and 6E). These anatomical studies reveal that $NMBR^+$ neurons in the sneeze-evoking region project directly to cVRG and synapse with neurons within cVRG.

The synaptic connections between $NMBR^+$ neurons and cVRG neurons are essential for signaling sneezing

cVRG contains mostly expiratory neurons that transmit excitatory drive to spinal motor neurons that control internal intercostal and abdominal expiratory muscles (Ezure et al., 2003; Iscoe, 1998; Shiba et al., 2007). To confirm the functional connections between $NMBR^+$ neurons and cVRG neurons, we tested whether cVRG neurons receive the synaptic input from $NMBR^+$ neurons by conducting electrophysiological recording of brainstem slices. Pharmacological activation of $NMBR^+$ neurons using NMB peptide evoked robust action potential (AP) firing in 30% of cVRG neurons (6 out of 20 neurons recorded; Figures 7A–7C). As a negative control, cVRG neurons in the brainstem slices from $Nmbr^{-/-}$ mice displayed no response to the same NMB treatment (0 out of 14 neurons recorded; Figures 7A and 7B). Our electrophysiological recordings confirm the

(K) Pain-related nose wiping behavior elicited by high-dose capsaicin (250 μM) remains intact in the $Nmb^{-/-}$ mice, as in WT mice.
(L) Capsaicin induces mouse apnea responses in a dose-dependent manner.
Each dot represents an individual mouse (n = 5–10 mice/group). Data are represented as mean ± SEM. **$p \leq 0.01$; ***$p \leq 0.001$; n.s, not significant. See also Figure S2.

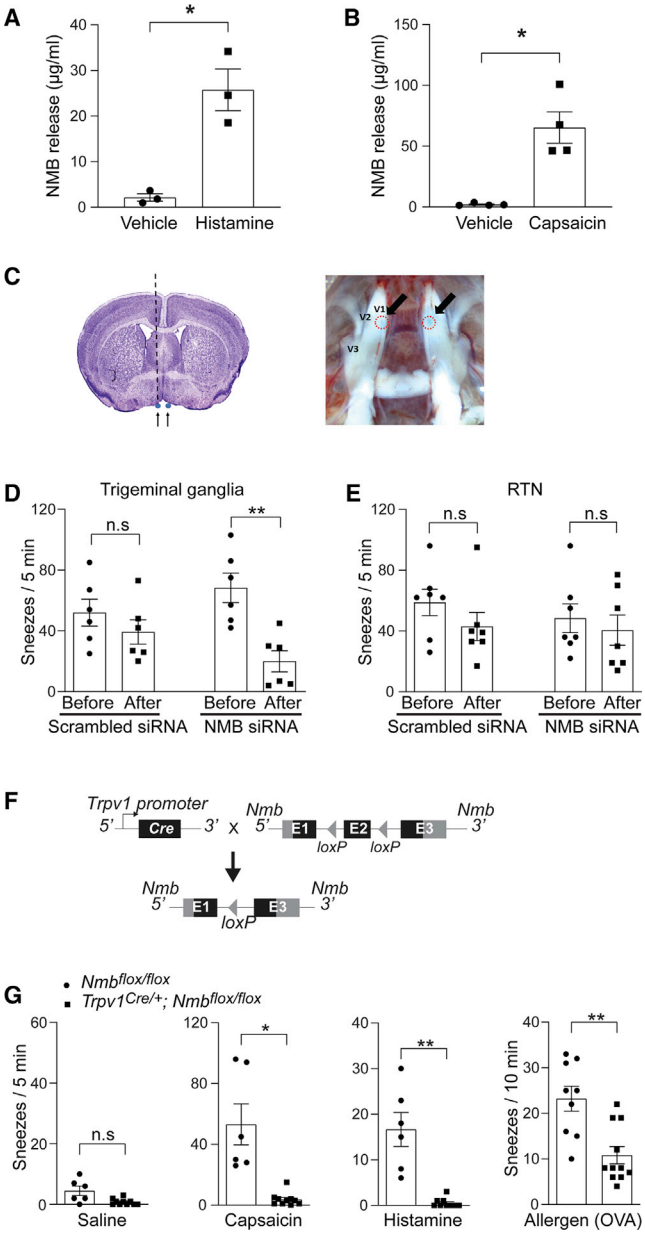

Figure 4. NMB is released from sensory neurons for signaling sneezing

(A and B) NMB is released from cultured TG neurons of WT mice after vehicle or sneeze-inducing compounds treatment (histamine, 200 μM; capsaicin, 10 μM). Each dot represents one replicate.

(C) Diagrams illustrating microinjection of siRNA into the V1 division of the TG. The black dotted line represents the path of the microinjection needle. Arrows in the right panel point toward the injection sites, outlined by red dashed circles, in the TG.

(D) NMB-siRNA silencing in the TG efficiently decreases the sneezing response to aerosolized capsaicin solution (12 μM) compared with the sneezing responses before microinjection or the nontargeting scrambled siRNA controls.

(E) NMB-siRNA silencing in the retrotrapezoid nucleus (RTN) does not affect the sneezing response to aerosolized capsaicin solution (12 μM).

(F) Schematic diagram illustrating the generation of *Trpv1*$^{Cre/+}$; *Nmb*$^{flox/flox}$ mice in which *Nmb* was conditionally knocked out in Trpv1-lineage sensory neurons.

functional connections between NMBR$^+$ neurons and cVRG neurons.

Since NMBR$^+$ neurons receive the sensory inputs from nasal sensory neurons, we further tested whether cVRG neurons are excited by sneeze-inducing stimuli. We activated sensory neurons using capsaicin and found that it elicited robust AP firing in 31.8% of cVRG neurons from WT mice (7 out of 22 neurons recorded; Figures 7D–7F) but weak or no AP firing from *Nmb*$^{-/-}$ mice (1 neuron with weak AP firing out of 13 neurons recorded; Figures 7D and 7E).

To determine the behavioral consequence of activating cVRG neurons via NMBR$^+$ axons, we microinjected NMB peptide directly into the cVRG region. *In vivo* activation of NMBR$^+$ axons innervating cVRG induces significant sneezing responses compared with the vehicle control (Figure 7G). Importantly, this sneeze-inducing effect was not observed in *Nmbr*$^{-/-}$ mice (Figure 7G), confirming the specificity of NMB for NMBR and NMBR$^+$ axons *in vivo*.

DISCUSSION

The sneezing reflex is beneficial to our health by rapidly removing noxious environmental irritants and pathogens from our airway. However, in the context of diseases, it can be annoying (e.g., hay fever) and even life-threatening in patients who are at high risk for lung herniation, subarachnoid hemorrhage, or aneurysm rupture (Baydin et al., 2005; Bradley et al., 1982; Brock and Heitmiller, 2000; Nomani et al., 2015). Sneezing also represents an important mechanism of disease transmission by generating and spreading huge numbers of infectious droplets. Despite its importance in medicine and public health, the neurophysiological mechanisms underlying sneezing have remained elusive.

Our study identifies the peptidergic neurotransmission pathway mediating the sneezing reflex (Figure 7H). Although the anatomical location of the sneeze-evoking region has been defined in the brainstems of both cats and humans (Hersch, 2000; Nonaka et al., 1990; Seijo-Martínez et al., 2006), it was unknown which neuronal population in this region signals sneezing. Using a reverse screening strategy, we reveal that NMBR$^+$ neurons are required for mediating sneezing induced by chemical irritants and allergens. This finding not only helps fill the gap in our knowledge of how the activation of nasal sensory fibers triggers the sneezing reflex but also provides a non-respiratory neuronal target for suppressing intractable pathological sneezing, without affecting normal respiration (Baydin et al., 2005; Bradley et al., 1982; Brock and Heitmiller, 2000; Nomani et al., 2015).

Although studies have shown the electrical activities of various respiratory neurons during fictive sneezing of cats (Batsel and Lines, 1978; Jakus et al., 1985; Orem and Brooks, 1986; Wallois et al., 1997), which respiratory population receives inputs from the sneeze-evoking region and drives sneezing remained unclear.

(G) *Trpv1*$^{Cre/+}$; *Nmb*$^{flox/flox}$ mice display significantly reduced sneezing responses to aerosolized capsaicin (12 μM), histamine (100 mM) solution, and chronic allergy induced by OVA (0.2 μg in 2 μL PBS/nostril).

Each dot represents an individual mouse (n = 6–11 mice/group). Data are represented as mean ± SEM. *p ≤ 0.05; **p ≤ 0.01; n.s, not significant. See also Figure S3.

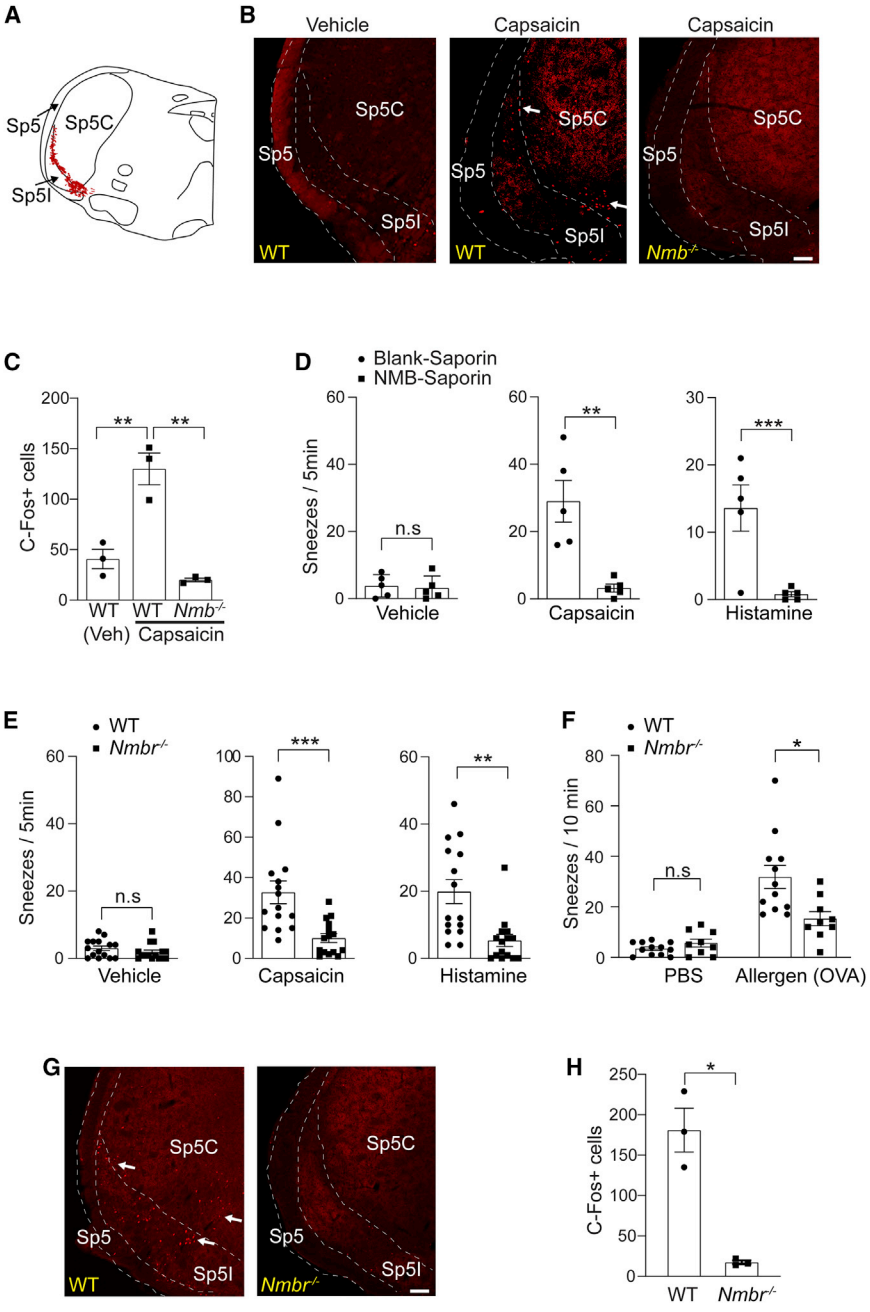

Figure 5. NMB-sensitive postsynaptic neurons in the sneeze-evoking region mediate sneezing

(A) Diagram showing the sneeze-evoking region (i.e., the central projection of nasal sensory neurons; indicated by red dots) in the spinal trigeminal nucleus (SpV) based on previous studies. Sp5, spinal trigeminal tract; Sp5C, spinal trigeminal nucleus caudalis; Sp5I, spinal trigeminal nucleus interpolar.

(B) Capsaicin-induced sneezes lead to a significant increase in the expression of c-Fos within the sneeze-evoking region of WT (indicated by arrows) compared with the saline vehicle control. *Nmb*-deficient mice display a significantly reduced c-Fos signal.

(C) Quantification of c-Fos$^+$ neurons in the sneeze-evoking region after saline (Veh) or capsaicin treatments.

(D) Microinjection of NMB-saporin into the sneeze-evoking region abolishes the sneezing responses to aerosolized capsaicin (12 μM) and histamine (100 mM) solution.

(E and F) *Nmbr*$^{-/-}$ mice display significantly reduced sneezing responses to aerosolized capsaicin (12 μM), histamine (100 mM) solution, and allergen (OVA 0.2 μg in 2 μL PBS/nostril) stimuli.

(G and H) Capsaicin-induced sneezes lead to the expression of c-Fos in the sneeze-evoking region of WT mice (indicated by arrows), but not *Nmbr*$^{-/-}$ mice.

All images shown are representatives of three biologically independent mice. Scale bars, 100 μm. The total number of c-Fos$^+$ neurons in the sneeze-evoking region was counted from 10 sections per mouse (n = 3 / genotype). Each dot represents an individual mouse. n = 5–15 mice/group for behavioral tests. Data are represented as mean ± SEM. *p ≤ 0.05; **p ≤ 0.01; ***p ≤ 0.001; n.s, not significant.

Our neuronal tracing and electrophysiological recordings reveal that NMBR$^+$ neurons synapse with cVRG expiratory neurons. Remarkably, *in vivo* activation of cVRG neurons via NMBR$^+$ axons induces significant sneezing responses. These results demonstrate that cVRG expiratory neurons are the direct projection target of NMBR$^+$ neurons in the sneeze-evoking region and are critically required for driving sneezing. However, the sneezing reflex involves both inspiratory and expiratory components. A future priority will be the integration of this peptidergic pathway with other respiratory neurons that influence sneezing. An interesting possibility is that NMBR$^+$ neurons may synapse with as-yet-unidentified interneurons that further regulate the activity of respiratory neurons controlling inspiration.

The newly defined sneezing pathway opens a door for future studies as to whether and how pathogens utilize our sneezing reflex to promote their propagation. We have shown that this peptidergic pathway mediates the sneezing responses to mast-cell-dependent allergy (see Figures 3H and 3I). By exploring published transcriptome data of human mast cells (Motakis et al., 2014), we found that mast cells express multiple receptors for respiratory virus, including ICAM-1 (the receptor for the majority of human rhinovirus), CD13/aminopeptidase N for several coronaviruses (e.g., prevalent human coronavirus-229E that causes common cold), and dipeptidyl peptidase IV for Middle East respiratory syndrome coronavirus (MERS-CoV) (Dijkman and van der Hoek, 2009; Greve et al., 1989; Li, 2015). It would be interesting to test

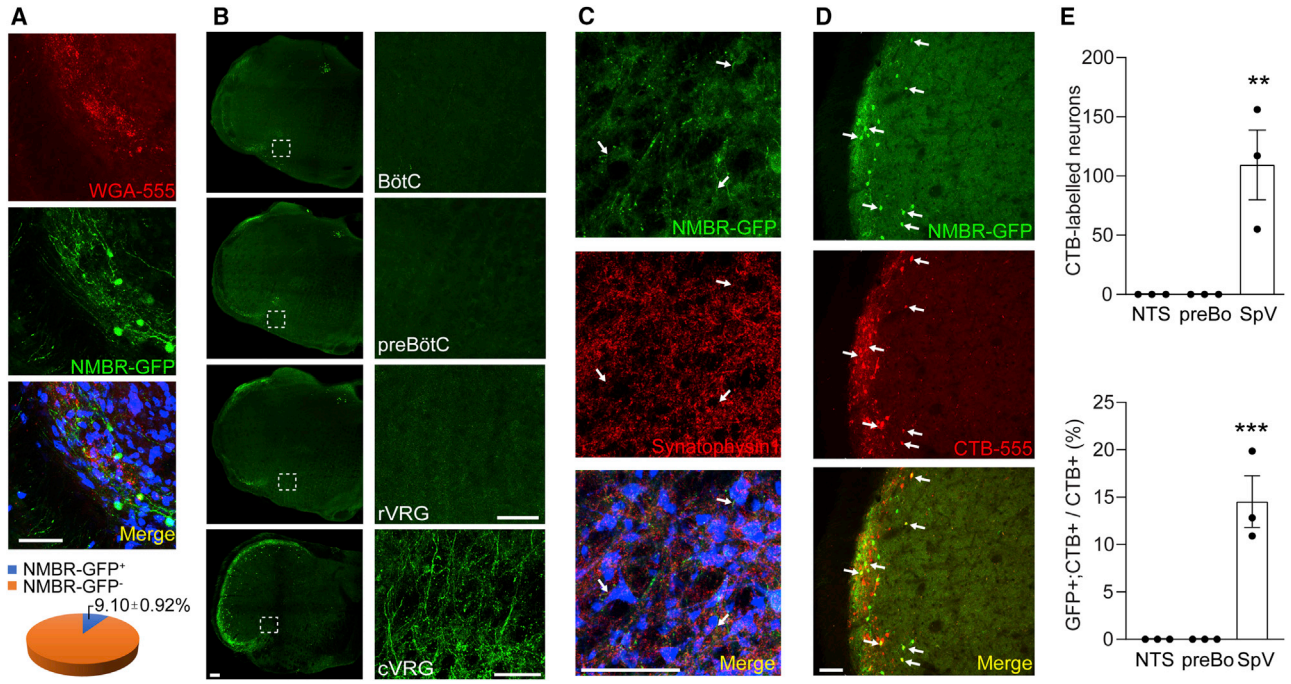

Figure 6. The projection of NMBR$^+$ neurons to the caudal ventral respiratory group

(A) Representative imaging of brainstem coronal sections showing that NMBR$^+$ neurons (green) comprise a highly restricted population in the sneeze-evoking region (red, labeled by WGA-555 applied to mouse nasal cavity). Neurons were marked by NeuN (blue).

(B) Representative imaging showing that NMBR$^+$ neurons selectively project to caudal ventral respiratory group (cVRG), but not other respiratory regions, including the rostral ventral respiratory group (rVRG), pre-Bötzinger complex (preBötC), and Bötzinger complex (BötC), as revealed by axonal tracing in *Nmbr*^{eGFP} reporter line. Images on the right show higher-magnification views of each boxed region.

(C) Representative imaging showing that NMBR-GFP$^+$ nerve fibers (green) express the presynaptic marker synaptophysin 1 (red) and synapse with cVRG neurons (marked by NeuN, blue).

(D and E) Retrograde axonal tracing by microinjection of CTB-555 into cVRG of *Nmbr*^{eGFP} mice shows that CTB-labeled NMBR-GFP$^+$ neurons (indicated by arrows) are localized within the sneeze-evoking region in the spinal trigeminal nucleus and absent from other brain regions, including the pre-Bötzinger complex (preBo) and nucleus tractus solitarius (NTS).

All images shown are representatives of three biologically independent mice. Scale bars, 100 μm. Each dot represents an individual mouse (n = 3 mice/group). Data are represented as mean ± SEM. **p ≤ 0.01; ***p ≤ 0.001. See also Figure S4.

whether these receptors mediate mast cell degranulation upon viral binding and result in the release of histamine or other mediators to trigger the sneezing reflex via this neural pathway.

In summary, our findings delineate the peptidergic pathway for chemically and allergy-induced sneezing (NMB$^+$ nasal sensory neurons → NMBR$^+$ neurons in the sneeze-evoking region → cVRG neurons) and have a direct and immediate impact on treating pathological sneezing and important implications in the fight against infectious respiratory diseases.

Limitations of the study

Our study reveals the neural pathway that mediates the sneezing reflex. A couple of limitations require further investigation. First, although we have shown that Trpv1$^+$/NMB$^+$ nasal sensory neurons initiate both chemically and allergy-induced sneezing, TrpV1 and NMB are expressed in several transcriptionally and functionally defined subtypes of primary sensory neurons. It is unclear which subset of Trpv1$^+$/NMB$^+$ nasal sensory neurons specifically encode sneezing. We recently identified a subset of Trpv1$^+$/NMB$^+$ nasal sensory neurons that detect mast cell mediators in allergic rhinitis and trigger the sneezing reflex. We are currently testing whether they are the long-sought neuronal population mediating sneezing. Second, as a defense mechanism, the sneezing reflex is not only induced by irritative chemicals and allergens as shown in this study but also triggered by mechanical stimuli, strong light, cold air, and viral infection. We are establishing mouse models for these types of sneezing so that we can investigate whether the identified peptidergic pathway mediates other types of sneezing. Findings from these studies will help determine whether different types of sneezing are mediated by a common neural pathway.

STAR★METHODS

Detailed methods are provided in the online version of this paper and include the following:

- KEY RESOURCES TABLE
- RESOURCE AVAILABILITY
  - Lead contact
  - Materials availability
  - Data and code availability

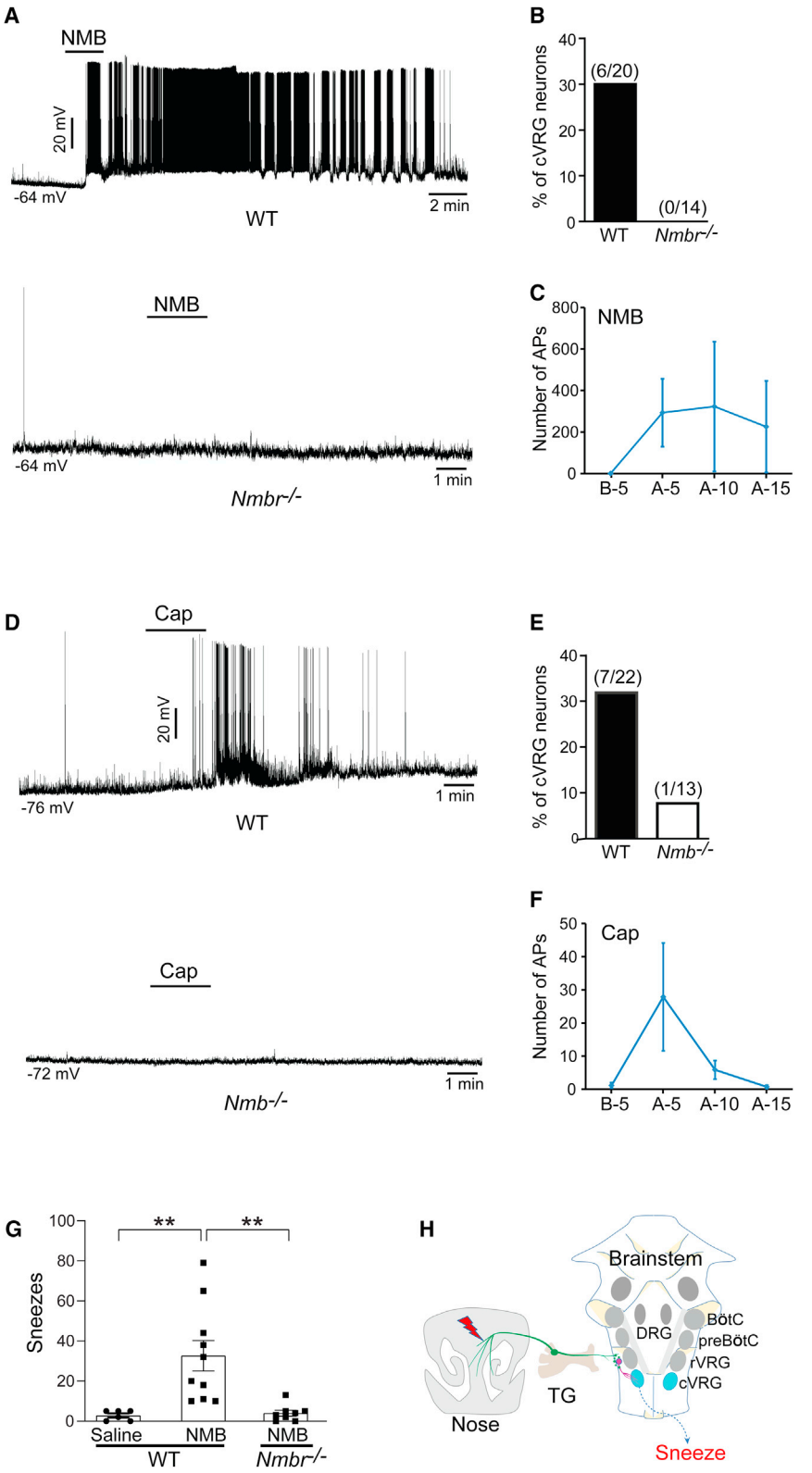

Figure 7. The synaptic connection between NMBR$^+$ neurons and cVRG neurons is essential for signaling sneezing

(A) Representative traces showing that pharmacological activation of NMBR$^+$ neurons using NMB peptide (4 μM) induces robust action potential (AP) firing in cVRG neurons of WT mice, but not *Nmbr*$^{-/-}$ mice.

(B) NMB peptide evokes robust AP firing in 30% of cVRG neurons recorded in the brainstem slices from WT mice. As a negative control, cVRG neurons of *Nmbr*$^{-/-}$ mice display no response to the same NMB treatment.

(C) The number of APs fired by WT cVRG neurons 5 min before (B-5) and 0–5 min (A-5), 5–10 min (A-10), and 10–15 min (A-15) after NMB treatment.

(D) Representative traces showing that capsaicin (5 μM) induces robust AP firing in cVRG neurons of WT mice, but not *Nmb*$^{-/-}$ mice.

(E) Capsaicin treatment elicits robust AP firing in 31.8% of cVRG neuron recorded from WT mice but weak or no AP firing from *Nmb*$^{-/-}$ mice.

(F) The number of APs fired by WT cVRG neurons 5 min before (B-5) and 0–5 min (A-5), 5–10 min (A-10), and 10–15 min (A-15) after capsaicin treatment.

(G) Microinjection of NMB peptide (1 pmol in 100 nL) into the cVRG region induces significant sneezing responses in WT mice, but not *Nmbr*$^{-/-}$ mice. As a control, microinjection of saline does not induce sneezing.

(H) Schematic diagram illustrating the neural pathway for sneezing (nasal NMB$^+$ sensory neurons → NMBR$^+$ neurons in the sneeze-evoking region → cVRG neurons). TG, trigeminal ganglia; rVRG, rostral ventral respiratory group; preBötC, pre-Bötzinger complex; BötC, Bötzinger complex; DRG, dorsal respiratory group.

Each dot represents an individual mouse (n = 6–10 mice/group). Data are represented as mean ± SEM. **p ≤ 0.01.

SUPPLEMENTAL INFORMATION

Supplemental information can be found online at https://doi.org/10.1016/j.cell.2021.05.017.

ACKNOWLEDGMENTS

We thank Qiufu Ma, Michael Panneton, Ru-Rong Ji, and Guo Huang for their helpful comments on the manuscript and Feixue Liang and Fengrui Zhang for their help with audio recording. This work was supported by the National Institutes of Health (grants R01AI125743 and R01EY024704) and the Pew Scholar Award (to Q.L.). B.S.K. is supported by NIAMS (grants K08-AR065577, R01AR070116, and R01AR077007), the American Skin Association, and the Doris Duke Charitable Foundation.

AUTHOR CONTRIBUTIONS

F.L. established the mouse sneezing model and performed behavioral tests, immunofluorescence staining, AEN bilateral rhizotomies, chemical ablation of Trpv1$^+$ nasal sensory fiber, allergic rhinitis model, cell picking, the NMB-siRNA study, neuronal ablation by NMB-saporin, genetic axonal tracing, retrograde neuronal tracing, NMB peptide microinjection into the cVRG, and data analysis and participated in paper preparation. H.J. performed behavioral tests, immunofluorescence staining, genetic axonal tracing, retrograde tracing, brainstem preparation, electrophysiological recordings, and data analysis and participated in paper preparation. X.S. performed behavioral tests, EMG recordings, immunofluorescence staining, retrograde tracing, and data analysis and participated in paper preparation. W.Y. performed chemical ablation of Trpv1$^+$ fibers, allergic rhinitis model, cell picking, sneezing and pain behavior assays, and data analysis. C.G. performed single-cell PCR assay and genetic mouse line generation. Z.W. conducted immunofluorescence staining. M.X. helped conduct sneezing behavioral tests. L.C. and W.L. conducted electrophysiological recordings and data analysis. Z.C. provided *Nmb*$^{-/-}$, *Nmbr*$^{-/-}$, and *Nmbr*$^{eGFP/+}$ mice and contributed to manuscript preparation. B.S.K. and A.J.W.H. contributed to experimental design and manuscript preparation. Q.L. planned and directed all the experiments and wrote the paper.

DECLARATION OF INTERESTS

The authors declare no competing interests. B.S.K. has noncompeting financial interests unrelated to this work and has served as a consultant for AbbVie, ABRAX Japan, Almirall, Cara Therapeutics, Maruho, Menlo Therapeutics, Pfizer, and Third Rock Ventures. He has participated on the advisory board for Almirall, Boehringer Ingelheim, Cara Therapeutics, Kiniksa Pharmaceuticals, Menlo Therapeutics, Regeneron Pharmaceuticals, Sanofi Genzyme, and Trevi Therapeutics. He is also founder, chief scientific officer, and stockholder of Nuogen Pharma and stockholder of Locus Biosciences.

Received: August 20, 2020
Revised: April 5, 2021
Accepted: May 12, 2021
Published: June 15, 2021

REFERENCES

Batsel, H.L., and Lines, A.J. (1978). Discharge of respiratory neurons in sneezes resulting from ethmoidal nerve stimulation. Exp. Neurol. *58*, 410–424.

Baydin, A., Nural, M.S., Güven, H., Deniz, T., Bildik, F., and Karaduman, A. (2005). Acute aortic dissection provoked by sneeze: a case report. Emerg. Med. J. *22*, 756–757.

Bourouiba, L. (2016). IMAGES IN CLINICAL MEDICINE. A Sneeze. N. Engl. J. Med. *375*, e15.

Bourouiba, L. (2020). Turbulent Gas Clouds and Respiratory Pathogen Emissions: Potential Implications for Reducing Transmission of COVID-19. JAMA *323*, 1837–1838.

Bourouiba, L., Dehandschoewercker, E., and Bush, J.W.M. (2014). Violent expiratory events: on coughing and sneezing. J. Fluid Mech. *745*, 27.

Bradley, W.G., Jr., Bank, W.O., and Fischbeck, K.H. (1982). Sneeze-induced hemiparesis from unruptured intracranial aneurysm. J. Neuroradiol. *9*, 323–327.

Brock, M.V., and Heitmiller, R.F. (2000). Spontaneous anterior thoracic lung hernias. J. Thorac. Cardiovasc. Surg. *119*, 1046–1047.

Caterina, M.J., Schumacher, M.A., Tominaga, M., Rosen, T.A., Levine, J.D., and Julius, D. (1997). The capsaicin receptor: a heat-activated ion channel in the pain pathway. Nature *389*, 816–824.

Cavanaugh, D.J., Chesler, A.T., Jackson, A.C., Sigal, Y.M., Yamanaka, H., Grant, R., O'Donnell, D., Nicoll, R.A., Shah, N.M., Julius, D., and Basbaum, A.I. (2011). Trpv1 reporter mice reveal highly restricted brain distribution and functional expression in arteriolar smooth muscle cells. J. Neurosci. *31*, 5067–5077.

Cole, E.C., and Cook, C.E. (1998). Characterization of infectious aerosols in health care facilities: an aid to effective engineering controls and preventive strategies. Am. J. Infect. Control *26*, 453–464.

Dell, R.B., Holleran, S., and Ramakrishnan, R. (2002). Sample size determination. ILAR J. *43*, 207–213.

Dijkman, R., and van der Hoek, L. (2009). Human coronaviruses 229E and NL63: close yet still so far. J. Formos. Med. Assoc. *108*, 270–279.

Doyle, W.J., Boehm, S., and Skoner, D.P. (1990). Physiologic responses to intranasal dose-response challenges with histamine, methacholine, bradykinin, and prostaglandin in adult volunteers with and without nasal allergy. J. Allergy Clin. Immunol. *86*, 924–935.

Ezure, K., Tanaka, I., and Saito, Y. (2003). Brainstem and spinal projections of augmenting expiratory neurons in the rat. Neurosci. Res. *45*, 41–51.

Feldman, J.L., Del Negro, C.A., and Gray, P.A. (2013). Understanding the rhythm of breathing: so near, yet so far. Annu. Rev. Physiol. *75*, 423–452.

Geppetti, P., Fusco, B.M., Marabini, S., Maggi, C.A., Fanciullacci, M., and Sicuteri, F. (1988). Secretion, pain and sneezing induced by the application of capsaicin to the nasal mucosa in man. Br. J. Pharmacol. *93*, 509–514.

Greve, J.M., Davis, G., Meyer, A.M., Forte, C.P., Yost, S.C., Marlor, C.W., Kamarck, M.E., and McClelland, A. (1989). The major human rhinovirus receptor is ICAM-1. Cell *56*, 839–847.

Han, F., Subramanian, S., Price, E.R., Nadeau, J., and Strohl, K.P. (2002). Periodic breathing in the mouse. J. Appl. Physiol. *92*, 1133–1140.

Han, L., Ma, C., Liu, Q., Weng, H.J., Cui, Y., Tang, Z., Kim, Y., Nie, H., Qu, L., Patel, K.N., et al. (2013). A subpopulation of nociceptors specifically linked to itch. Nat. Neurosci. *16*, 174–182.

Hersch, M. (2000). Loss of ability to sneeze in lateral medullary syndrome. Neurology *54*, 520–521.

Hydén, D., and Arlinger, S. (2007). On the sneeze-reflex and its control. Rhinology *45*, 218–219.

Iscoe, S. (1998). Control of abdominal muscles. Prog. Neurobiol. *56*, 433–506.

Jakus, J., Tomori, Z., and Stránsky, A. (1985). Activity of bulbar respiratory neurones during cough and other respiratory tract reflexes in cats. Physiol. Bohemoslov. *34*, 127–136.

Karai, L., Brown, D.C., Mannes, A.J., Connelly, S.T., Brown, J., Gandal, M., Wellisch, O.M., Neubert, J.K., Olah, Z., and Iadarola, M.J. (2004). Deletion of vanilloid receptor 1-expressing primary afferent neurons for pain control. J. Clin. Invest. *113*, 1344–1352.

Kumar, P., Wu, H., McBride, J.L., Jung, K.E., Kim, M.H., Davidson, B.L., Lee, S.K., Shankar, P., and Manjunath, N. (2007). Transvascular delivery of small interfering RNA to the central nervous system. Nature *448*, 39–43.

Kushnir-Sukhov, N.M., Brown, J.M., Wu, Y., Kirshenbaum, A., and Metcalfe, D.D. (2007). Human mast cells are capable of serotonin synthesis and release. J. Allergy Clin. Immunol. *119*, 498–499.

Lee, M.G., Dong, X., Liu, Q., Patel, K.N., Choi, O.H., Vonakis, B., and Undem, B.J. (2008). Agonists of the MAS-related gene (Mrgs) orphan receptors as novel mediators of mast cell-sensory nerve interactions. J. Immunol. *180*, 2251–2255.

Li, F. (2015). Receptor recognition mechanisms of coronaviruses: a decade of structural studies. J. Virol. *89*, 1954–1964.

Li, P., Janczewski, W.A., Yackle, K., Kam, K., Pagliardini, S., Krasnow, M.A., and Feldman, J.L. (2016). The peptidergic control circuit for sighing. Nature *530*, 293–297.

Li, F., Yang, W., Jiang, H., Guo, C., Huang, A.J.W., Hu, H., and Liu, Q. (2019). TRPV1 activity and substance P release are required for corneal cold nociception. Nat. Commun. *10*, 5678.

Liu, Q., Vrontou, S., Rice, F.L., Zylka, M.J., Dong, X., and Anderson, D.J. (2007). Molecular genetic visualization of a rare subset of unmyelinated sensory neurons that may detect gentle touch. Nat. Neurosci. *10*, 946–948.

Lucier, G.E., and Egizii, R. (1986). Central projections of the ethmoidal nerve of the cat as determined by the horseradish peroxidase tracer technique. J. Comp. Neurol. *247*, 123–132.

McCoy, E.S., Taylor-Blake, B., and Zylka, M.J. (2012). CGRPα-expressing sensory neurons respond to stimuli that evoke sensations of pain and itch. PLoS ONE *7*, e36355.

Mishra, S.K., Tisel, S.M., Orestes, P., Bhangoo, S.K., and Hoon, M.A. (2011). TRPV1-lineage neurons are required for thermal sensation. EMBO J. *30*, 582–593.

Mishra, S.K., Holzman, S., and Hoon, M.A. (2012). A nociceptive signaling role for neuromedin B. J. Neurosci. *32*, 8686–8695.

Motakis, E., Guhl, S., Ishizu, Y., Itoh, M., Kawaji, H., de Hoon, M., Lassmann, T., Carninci, P., Hayashizaki, Y., Zuberbier, T., et al.; FANTOM consortium (2014). Redefinition of the human mast cell transcriptome by deep-CAGE sequencing. Blood *123*, e58–e67.

Nomani, A.Z., Rajput, H.M., Iqbal, M., Jan, Z., Irshad, M., Badshah, M., and Khan, R.S. (2015). Subarachnoid hemorrhage secondary to forceful sneeze. Case Rep. Neurol. Med. *2015*, 896732.

Nonaka, S., Unno, T., Ohta, Y., and Mori, S. (1990). Sneeze-evoking region within the brainstem. Brain Res. *511*, 265–270.

Orem, J., and Brooks, E.G. (1986). The activity of retrofacial expiratory cells during behavioral respiratory responses and active expiration. Brain Res. *374*, 409–412.

Panneton, W.M., Gan, Q., and Juric, R. (2006). Brainstem projections from recipient zones of the anterior ethmoidal nerve in the medullary dorsal horn. Neuroscience *141*, 889–906.

Satoh, I., Shiba, K., Kobayashi, N., Nakajima, Y., and Konno, A. (1998). Upper airway motor outputs during sneezing and coughing in decerebrate cats. Neurosci. Res. *32*, 131–135.

Scharfman, B.E., Techet, A.H., Bush, J.W.M., and Bourouiba, L. (2016). Visualization of sneeze ejecta: steps of fluid fragmentation leading to respiratory droplets. Exp. Fluids *57*, 24.

Seijo-Martínez, M., Varela-Freijanes, A., Grandes, J., and Vázquez, F. (2006). Sneeze related area in the medulla: localisation of the human sneezing centre? J. Neurol. Neurosurg. Psychiatry *77*, 559–561.

Shiba, K., Nakazawa, K., Ono, K., and Umezaki, T. (2007). Multifunctional laryngeal premotor neurons: their activities during breathing, coughing, sneezing, and swallowing. J. Neurosci. *27*, 5156–5162.

Shim, W.S., Tak, M.H., Lee, M.H., Kim, M., Kim, M., Koo, J.Y., Lee, C.H., Kim, M., and Oh, U. (2007). TRPV1 mediates histamine-induced itching via the activation of phospholipase A2 and 12-lipoxygenase. J. Neurosci. *27*, 2331–2337.

Songu, M., and Cingi, C. (2009). Sneeze reflex: facts and fiction. Ther. Adv. Respir. Dis. *3*, 131–141.

Tang, J.W., Li, Y., Eames, I., Chan, P.K., and Ridgway, G.L. (2006). Factors involved in the aerosol transmission of infection and control of ventilation in healthcare premises. J. Hosp. Infect. *64*, 100–114.

Taylor-Clark, T.E., Kollarik, M., MacGlashan, D.W., Jr., and Undem, B.J. (2005). Nasal sensory nerve populations responding to histamine and capsaicin. J. Allergy Clin. Immunol. *116*, 1282–1288.

Tønnesen, P., and Mygind, N. (1985). Nasal challenge with serotonin and histamine in normal persons. Allergy *40*, 350–353.

Uzzaman, A., and Story, R. (2012). Chapter 5: Allergic rhinitis. Allergy Asthma Proc. *33* (*Suppl 1*), 15–18.

Wada, E., Way, J., Lebacq-Verheyden, A.M., and Battey, J.F. (1990). Neuromedin B and gastrin-releasing peptide mRNAs are differentially distributed in the rat nervous system. J. Neurosci. *10*, 2917–2930.

Wada, E., Way, J., Shapira, H., Kusano, K., Lebacq-Verheyden, A.M., Coy, D., Jensen, R., and Battery, J. (1991). cDNA cloning, characterization, and brain region-specific expression of a neuromedin-B-preferring bombesin receptor. Neuron *6*, 421–430.

Wallois, F., Macron, J.M., Jounieaux, V., and Duron, B. (1991). Trigeminal afferences implied in the triggering or inhibition of sneezing in cats. Neurosci. Lett. *122*, 145–147.

Wallois, F., Bodineau, L., Macron, J.M., Marlot, D., and Duron, B. (1997). Role of respiratory and non-respiratory neurones in the region of the NTS in the elaboration of the sneeze reflex in cat. Brain Res. *768*, 71–85.

Wan, L., Jin, H., Liu, X.Y., Jeffry, J., Barry, D.M., Shen, K.F., Peng, J.H., Liu, X.T., Jin, J.H., Sun, Y., et al. (2017). Distinct roles of NMB and GRP in itch transmission. Sci. Rep. *7*, 15466.

Williams, W.O., Riskin, D.K., and Mott, A.K. (2008). Ultrasonic sound as an indicator of acute pain in laboratory mice. J. Am. Assoc. Lab. Anim. Sci. *47*, 8–10.

Yamauchi, M., Dostal, J., Kimura, H., and Strohl, K.P. (2008a). Effects of buspirone on posthypoxic ventilatory behavior in the C57BL/6J and A/J mouse strains. J. Appl. Physiol. *105*, 518–526.

Yamauchi, M., Ocak, H., Dostal, J., Jacono, F.J., Loparo, K.A., and Strohl, K.P. (2008b). Post-sigh breathing behavior and spontaneous pauses in the C57BL/6J (B6) mouse. Respir. Physiol. Neurobiol. *162*, 117–125.

Zhao, Z.Q., Wan, L., Liu, X.Y., Huo, F.Q., Li, H., Barry, D.M., Krieger, S., Kim, S., Liu, Z.C., Xu, J., et al. (2014). Cross-inhibition of NMBR and GRPR signaling maintains normal histaminergic itch transmission. J. Neurosci. *34*, 12402–12414.

STAR★METHODS

KEY RESOURCES TABLE

REAGENT or RESOURCE	SOURCE	IDENTIFIER
Antibodies		
Rabbit anti-GFP	Invitrogen	Cat#A-11122; RRID: AB_221569; Lot#1925070
Chicken anti-GFP	Aves	Cat#GFP-1020; RRID: AB_2307313 Lot#879484
Rabbit anti-c-Fos	Santa Cruz Biotechnology	Cat#sc-52; Lot#B0112
Guinea pig anti-Synaptophysin 1	Synaptic System	Cat#101004
Mouse anti-NeuN	MilliporeSigma	Cat#MAB377; Lot#3205920
Goat anti-Wheat Germ Agglutinin (WGA)	Vector Laboratories	Cat#AS-2024; Lot#T1112
Rabbit anti-PGP9.5	Abcam	Cat#ab10404
Goat anti-rabbit IgG-Alexa Fluor-488	Invitrogen	Cat#A-11008; RRID: AB_143165; Lot#1797971
Alexa Fluor 488 AffiniPure F(ab')$_2$ Fragment Donkey Anti-Chicken IgY (IgG) (H+L)	Jackson ImmunoResearch	Cat#703-546-155; RRID: AB_2340376; Lot#147291
Goat anti-rabbit IgG-Alexa Fluor-555	Invitrogen	Cat#A-21429; RRID: AB_2535850; Lot#1683674
Goat anti-guinea pig IgG-Alexa Fluor-555	Invitrogen	Cat#A-21435; RRID: AB_2535856;
Cy3 AffiniPure Donkey Anti-Goat IgG	Jackson ImmunoResearch	Cat#705-165-147; RRID: AB_2307351; Lot#148575
Goat anti-mouse IgG-Alexa Fluor-Cyanine5	Invitrogen	Cat#A10524; RRID: AB_2534033;
Chemicals, peptides, and recombinant proteins		
Capsaicin	Sigma-Aldrich	Cat#M2028; CAS: 404-86-4
Histamine dihydrochloride	Sigma-Aldrich	Cat#H7250; CAS: 56-92-8;
Serotonin	Sigma-Aldrich	Cat#H9523; CAS: 153-98-0
Neuropeptide FF	BACHEM	Cat#H-5655.0001; CAS: 99566-27-5
Ovalbumin	Sigma-Aldrich	Cat#A5503; CAS: 9006-59-1
Imject Alum Adjuvant	Thermo Scientific	Cat#77161
Resiniferatoxin	Sigma-Aldrich	Cat#R8756; CAS: 57444-62-9
OCT	Sakura	Cat#4583
Nitrotetrazolium Blue chloride	Sigma-Aldrich	Cat#N6876; CAS: 298-83-9
5-bromo-4-chloro-3-indolyl phosphate disodium salt	Sigma-Aldrich	Cat#B6149; CAS: 102185-33-1
WGA-Alexa Fluor 488	Molecular Probes	Cat#W11261
WGA-Alexa Fluor 555	Molecular Probes	Cat#W32464
HotStarTaq DNA Polymerase	QIAGEN	Cat#203203
RVG-9R	BACHEM	Cat#H-7502.0500; CAS: 1678417-57-6
NMB-saporin	Advanced Targeting Systems	Cat#IT-70
Blank-saporin	Advanced Targeting Systems	Cat#IT-21
Alexa 555 conjugated cholera toxin subunit B	Invitrogen	Cat#C34776;
NMB peptide	TOCRIS	Cat#1908
Bovine Serum Albumin	Fisher BioReagents	Cat#BP9706-100
Critical commercial assays		
SuperScript III CellsDirect cDNA Synthesis Kit	Invitrogen	Cat#18080200
Mouse NMB / Neuromedin B (Competitive EIA) ELISA Kit	LifeSpan Biosciences	Cat#LS-F4262

(*Continued on next page*)

Continued

REAGENT or RESOURCE	SOURCE	IDENTIFIER
Experimental models: cell lines		
HEK293 cells	ATCC	CRL-1573
Experimental models: organisms/strains		
Mouse: C57BL/6J	Jackson Laboratory	Stock#000664
Mouse: *Trpv1*$^{PLAP\text{-}nlacZ}$	Jackson Laboratory	Stock#017623
Mouse: *Vglut2*^{FLOX}	Jackson Laboratory	Stock#012898
Mouse: *Tac1*$^{-/-}$	Jackson Laboratory	Stock#004103
Mouse: *Kit*$^{W\text{-}sh/HNihrJaeBsm}$/*J*	Jackson Laboratory	Stock#005051
Mouse: *Trpv1*^{Cre}	Mark Hoon (NIDCR)	Mishra et al., 2011
Mouse: *Nmb*$^{flox/flox}$	The Molecular Genetic Service Core of the Department of Ophthalmology and Visual Science at Washington University in St. Louis	N/A
Mouse: *Calca*$^{-/-}$	Mark Zykla (University of North Carolina)	McCoy et al., 2012
Mouse: *Nmb*$^{-/-}$	Zhou-Feng Chen (Washington University in St. Louis)	Wan et al., 2017
Mouse: *Nmbr*$^{-/-}$	Zhou-Feng Chen (Washington University in St. Louis)	Wan et al., 2017; Zhao et al., 2014
Mouse: *Nmbr*$^{eGFP/+}$	Zhou-Feng Chen (Washington University in St. Louis)	Wan et al., 2017; Zhao et al., 2014
Oligonucleotides		
siRNA targeting *Nmb*	Dharmacon	Cat#M-046334-01-0005
Nontargeting scrambled controls	Dharmacon	Cat#D-001206-14-05
Primers for single cell RT-PCR, see Table S2	This paper	N/A
Recombinant DNA		
Nmb expression constructs	OriGene Technologies	MR200598
Software and algorithms		
FinePointe Software	DSI	007898-001 Rev03
Audacity	Audacity Team	https://www.audacityteam.org/
Adobe Premiere Pro 2020	Adobe	https://www.adobe.com/products/premiere.html
MATLAB	Mathworks	https://www.mathworks.com/products/matlab.html
LabScribe software	iWorx Systems	Sn#R27196
pClamp 10.5	Molecular Devices	https://support.moleculardevices.com/s/article/Axon-pCLAMP-10-Electrophysiology-Data-Acquisition-Analysis-Software-Download-Page
Prisim 8	Graphpad	https://www.graphpad.com:443/scientific-software/prism/
Other		
Whole Body Plethysmography System	DSI	601-1400-001 Rev11
Ultrasonic nebulizer	DSI	08271-001
Mesh Type Nebulizer	OMRON	Model NE-U22
Video camera	Canon	VIXIA HFG10
Small voice recorder (16 kHz)	aTTo digital	N/A
Microphone	Bruel & Kjaer	Type 4134
BNC-2110 recorder	National Instruments	N/A
LabVIEW	National Instruments	N/A

(*Continued on next page*)

Continued

REAGENT or RESOURCE	SOURCE	IDENTIFIER
I/O ports of data acquisition cards	National Instruments	PCI-6731 and PCI-4052e
IX-BIO8 biopotential recorder	iWorx Systems	Sn#R27196
Zone-Quick diagnostic threads	Menicon	N/A
DMi6000 inverted epifluorescence microscope	Leica	N/A
MMO-202ND micromanipulator	Narishige	N/A
Glass-bottomed culture dish	MatTek Corporation	Part#P35G-1.5-7-C
Digital Stereotaxic apparatus	Leica	Model#39477001
Neuros-syringe	Hamilton	N/A
SMARTouch controller	World Precision Instruments	Model 40220
Vibratome Series 3000 Plus Tissue Sectioning System	Vibratome	N/A
MultiClamp 700B amplifier	Molecular Devices	N/A

RESOURCE AVAILABILITY

Lead contact

Further information and requests for resources and reagents should be directed to and will be fulfilled by the lead contact, Qin Liu (qinliu@wustl.edu).

Materials availability

This study did not generate new unique reagents.

Data and code availability

This study did not generate datasets/code.

EXPERIMENTAL MODEL AND SUBJECT DETAILS

Mouse lines

C57BL/6J wild-type (Stock#: 000664), *Trpv1*$^{PLAP\text{-}nlacZ}$ (Stock#: 017623), *Vglut2*^{FLOX} (Stock#: 012898), *Tac1*$^{-/-}$ (Stock#: 004103) and *Kit*$^{W\text{-}sh/HNihrJaeBsm}$*/J* (Stock#: 005051) mice were ordered from the Jackson Laboratory. *Trpv1*^{Cre} mice were gifted by Dr. Mark Hoon at the NIDCR (Mishra et al., 2011). *Nmb*$^{flox/flox}$ mice were generated using ES cells from the European Conditional Mouse Mutagenesis Program (EUCOMM) by the Molecular Genetic Service Core of the Department of Ophthalmology and Visual Science at Washington University in St. Louis. *Calca*$^{-/-}$ mice were gifted by Dr. Mark Zykla at the University of North Carolina (McCoy et al., 2012). *Nmb*$^{-/-}$, *Nmbr*$^{-/-}$ and *Nmbr*$^{eGFP/+}$ mice were provided by Dr. Zhou-Feng Chen at Washington University Center for the Study of Itch and Sensory Disorders (Wan et al., 2017; Zhao et al., 2014).

All experiments were performed in accordance with protocols approved by the Institutional Animal Care and Use Committee at Washington University in Saint Louis, School of Medicine. All animals used in this study were housed on a 12:12 hour light cycle with *ad libitum* access to food and water. Three- to eight-week-old animals used for tissue collection, histology, and electrophysiological recordings. For behavioral experiments and electromyogram recording, all animals were between 8-12 weeks old at the time of testing. *C57BL/6J* wild-type mice were randomly assigned to control and treatment groups. Transgenic and control mice were assigned to groups based on their genotype. Researchers were blinded to treatment and mouse genotypes throughout testing and data analysis. Both male and female mice were used for electromyogram recording, tissue collection, histology, and electrophysiological recordings. No significant sex related differences were observed or noted.

METHOD DETAILS

Sneezing behavior study

Sneezing responses in mice were recorded using Buxco Small Animal Whole Body Plethysmography System (DSI, 601-1400-001 Rev11) and analyzed using the FinePointe Software (DSI, 007898-001 Rev03). Test animals were placed in the recording chamber for 10 minutes for acclimation and baseline testing. For chemical-induced sneezing, 0.3 mL of test solution were delivered using an ultrasonic nebulizer (DSI, 08271-001) over 2 min. Reagents used include histamine (Sigma, H7250), capsaicin (Sigma, M2028), and serotonin (Sigma, H9523). NPFF (BACHEM, H-5655.0001, 20 nmol in 2 μl saline) was instilled into each nostril of test mice. Sneezing behavior was recorded for 5 to 10 min. Sneezes, characterized by forceful expirations, were identified from the respiratory trace

generated by the FinePointe Software of the WBP system. Apnea was defined as an end-expiratory pause of $\geq$ 2 average breath durations as in previous studies (Han et al., 2002; Yamauchi et al., 2008a, 2008b). For video and audio recordings, a video camera (Canon, VIXIA HFG10) was placed on the top of the recording chamber. For simultaneous WBP and audio recordings, a mini audio recorder (aTTo digital, 16 kHz) was placed into the WBP recording chamber. Audio component was extracted from video files and analyzed using the software Audacity.

Ultrasonic recordings were conducted inside an audiometric booth. For mouse sneeze recordings, Microphone (Bruel & Kjaer, type 4134) was adjusted near the snout of the test mouse. For tail snip induced vocalization, mice were gently restrained close to the microphone (Williams et al., 2008). All sound recordings were collected using the BNC-2110 recorder (National Instruments), which is sensitive to frequencies up to 100 kHz, and were written in LabVIEW (National Instruments) consisted of I/O ports of data acquisition cards (PCI-6731 and PCI-4052e, National Instruments) and peripheral circuits. Sound signals were analyzed using MATLAB.

Mast cell-dependent allergy in mice was adapted from our previous study (Han et al., 2013). In brief, 0.02% ovalbumin (OVA, Sigma, A5503) in sterile PBS (w/vol) was emulsified with an equal volume of Imject Alum (Thermo Scientific, 77161). Mice received *i.p.* injection of 200 μL OVA/Imject Alum mixture on the 1st and 11th day. For acute allergic model, sneezing responses were recorded for 10 min after nasal challenge with OVA (2 μL, 10%) on day 14. For chronic allergic model, sensitized animals were challenged daily with intranasal instillation of OVA (2 μL, 10%) under isoflurane anesthesia for five days (from day 14 to 18). Sneezing responses were tested immediately after nasal challenge with OVA on day 19.

Anterior ethmoidal nerve (AEN) bilateral rhizotomies

Rhizotomy of mouse AEN was performed using an intra-orbital approach as previously described (Panneton et al., 2006). Briefly, anesthetized adult mice were secured in a custom-made stereotaxic apparatus to immobilize the head during the procedure. A dorsal incision was made in the skin from bregma to the anterior of the nose to expose both sides of the medialis orbits. The AEN was seen entering the anterior ethmoidal foramen medially after retracting the eyeball laterally. Rhizotomy was accomplished after careful isolation of the AEN nerve. In the sham group, AEN was isolated without rhizotomy. After the surgery, mice were provided buprenorphine-SR (0.5 mg/kg *s.c,* once) and carprofen (5 mg/kg *i.p,* every eight hours for one day) for pain relief. Sneezing reflexes were tested two weeks after surgery.

Electromyogram recording of sneeze-related muscle movement

Electromyogram (EMG) recording of sneeze-related muscle movement was conducted according to the protocol adapted from a previous study (Satoh et al., 1998). Using IX-BIO8 biopotential recorder and LabScribe software (iWorx Systems Inc., Sn#R27196), EMGs were recorded in anesthetized adult mice via bipolar stainless steel wire electrodes implanted into the diaphragm and external oblique abdominus, respectively. Anesthesia depth was set at a level where animals were fully restrained but still produced sneezing-related muscle movements in response to nasal mechanical stimulation. Muscle movements were recorded for three minutes after saline or capsaicin (12 μM) challenges. To measure muscle activity, EMG signals sampled at 1000 Hz were digitally rectified and integrated. Muscular contractions that significantly increase over regular respiratory movement and interrupt the respiratory rhythm were counted as sneezing-related responses as described in previous study (Satoh et al., 1998).

Chemical ablation or desensitization of Trpv1$^+$ nasal sensory fiber

To degenerate or desensitize Trpv1$^+$ fibers from the nose, resiniferatoxin (Sigma, R8756, 50 ng in 2 μL saline) or capsaicin (Sigma, M2028, 60 ng in 2 μL saline) was instilled into each nostril of ketamine/xylazine anesthetized mice. Sneezing behavior was tested five days after resiniferatoxin treatments and two days after capsaicin treatments.

Nasal secretion

Nasal secretions of adult mice were tested using phenol red thread (PRT) tests. Three minutes after saline or capsaicin (12 μM) challenge, Diagnostic threads (Zone-Quick, Menicon Co., Ltd) were placed inside the nostril for 15 s. The absorption of nasal mucus fluid by the thread was measured by the length of the color change (due to pH change) as indicated by the manual.

Histochemistry study of nasal sensory fibers

Adult mice were anesthetized with ketamine/xylazine cocktail and transcardially perfused with PBS, followed by 4% paraformaldehyde (PFA) in PBS (w/vol). The nose was dissected by trimming away the lower jaw and surrounding tissues, then post-fixed in 4% PFA on ice for 2 hours. The nasal tissue was incubated in a decalcification buffer (250 mM EDTA in 30% sucrose/PBS) for two days at 4°C, with buffer changes every 12 hours. After decalcification, the nose was immersed in OCT (Sakura, 4583) and placed in a vacuum chamber for 2 hours to allow OCT to fill the nasal cavity. Afterward, embedded nose tissues were frozen for sectioning. For PGP9.5 staining, nose sections were blocked in 10% goat serum (vol/vol) for 1 hour and incubated with the primary antibody rabbit anti-PGP9.5 (Abcam, ab10404; 1:1000 in 0.2% PBST) solution overnight at 4°C. After rinse, the sections were incubated with the secondary antibody anti-Rabbit IgG - Alexa Fluor 488 (Invitrogen, A11008, Lot# 1797971; 1:500 in 0.2% PBST) for 2 hours at room temperature.

Trpv1-PLAP staining was adapted from our previous study (Liu et al., 2007). Briefly, nose sections were fixed in 4% PFA for 10 min on ice and rinsed with HBSS before PLAP staining. Endogenous alkaline phosphatase activity was blocked by incubation at 65°C in

HBSS for 2 hours. After incubation, slides were washed in sequence with HBSS, B1 buffer (0.1 M Tris pH 7.5, 0.15 M NaCl), and freshly prepared B3 buffer (0.1 M Tris pH 9.5, 0.1 M NaCl, 50 mM $MgCl_2$). PLAP activity was then visualized by incubation with 37.5 μg/mL nitrotetrazolium blue chloride (Sigma, N6876), 175 μg/mL 5–bromo-4-chloro-3-indolyl phosphate disodium salt (Sigma, B6149) in B3 buffer at room temperature until signals appeared. PLAP reaction was stopped by rinsing the sections in HBSS and fixed in 4% PFA at 4°C for 4 hours.

Retrograde labeling and single cell RT-PCR

Adult mice were anesthetized using ketamine/xylazine cocktail and were placed under a stereoscopic microscope. Intranasal instillation of WGA-Alexa Fluor 488 (10 μg in 2 μL PBS, Molecular Probes, W11261) was performed using a fine glass capillary. Trigeminal ganglia were dissected and dissociated two days after instillation. Neurons were purified using a 15% BSA density gradient column as previously described (Li et al., 2019). WGA labeled cells were isolated manually using a custom made cell-picking setup comprising of a Leica DMi6000 inverted epifluorescence microscope (Buffalo Grove, IL) and a Narishige MMO-202ND micromanipulator (Amityville, NY). WGA labeled cells were identified visually under the microscope, captured, ejected into PCR tubes containing 10 μL of lysis buffer and RNase inhibitor (Invitrogen, 18080200), and flash frozen and stored at −80°C until cDNA synthesis.

cDNA was generated using Invitrogen SuperScript III CellsDirect cDNA Synthesiss Kit (Invitrogen, 18080200) according to the manufacturer's recommended protocol. DNase digestion was performed for all samples. RT-PCR was performed using 2 μL of cDNA and QIAGEN HotStarTaq Polymerase (QIAGEN, 203203). Genomic DNA, obtained from single neuron, was used as the negative control. cDNA from whole trigeminal ganglion lysate was used as the positive control. Gene specific primers and annealing temperatures are listed in the Table S2.

Capsaicin pain behavior

Mice were acclimated in the recording chamber for 30 min before treatment. Capsaicin solution (0.5 nmol in 2 μL saline) was instilled into each nostril. Wiping behavior was videotaped for 5 min immediately after instillation.

Enzyme-linked immunosorbent assay (ELISA)

To detect NMB release from sensory neurons, TG neurons were dissociated and seeded at high density on the 7 mm glass window of a glass-bottomed culture dish (MatTek Corporation). Neurons were cultured at 37°C for 24 hours and were gently rinsed twice with warm Ca^{2+}- and Mg^{2+}-free HBSS before test. To activate the neurons, 50 μL of CIB containing vehicle or stimulants were gently added onto the neurons and incubated at 37°C for 5 min before the supernatant was collected. NMB concentration in the supernatant was then measured by ELISA (LifeSpan Biosciences, Cat#:LS-F4262) using the manufacturer's supplied standards and their recommended protocol.

NMB-siRNA study

siRNA knockdown efficiency was evaluated using HEK293 cells transfected with *Nmb* plasmid (OriGene Technologies, MR200598). 200ng of plasmid with either *Nmb*-siRNA (15 pmol in 250 μL, M-046334-01-0005, Dharmacon) or scramble-siRNA (15 pmol in 250 μL, D-001206-14-05, Dharmacon) were co-transfected into HEK293 cells. 24 hours after transfection, *Nmb* mRNA expression was quantified by RT-qPCR.

In vivo knockdown of *Nmb* was accomplished using siRNA microinjections. All injections were performed in ketamine/xylazine anesthetized mice using a Digital Stereotaxic apparatus (Leica, Model# 39477001). 5 μL of 0.4 μg/μL siRNA targeting *Nmb* (Dharmacon, M-046334-01-0005) or nontargeting scrambled controls (Dharmacon, D-001206-14-05) in nuclease free water were mixed with 5 μL of 1.45 μg/μL RVG-9R (Bachem, H-7502.0500) (Kumar et al., 2007) in 10% glucose and incubated at room temperature for 20 min. After incubation, the siRNA/RVG mixture (200 nL) was injected into the V1 division of trigeminal ganglion or retrotrapezoid nucleus region via a custom-made 32 gauge, 500 nL neuros-syringe (Hamilton Co.) controlled by a SMARTouch controller (World Precision Instruments, Model 40220); and repeated on the contralateral side. Coordinates for V1 division were: 0.7 mm anterior to bregma, 6.0 mm ventral from surface, ± 1.5 mm from midline. Coordinates for retrotrapezoid nucleus region were: 6.4 mm posterior to bregma, 4.75 mm ventral from surface, ± 1.3 mm from midline. Sneezing responses were tested 4 days after siRNA injection.

Immunofluorescence staining of the brainstem

Brainstems of mice were collected after 4% PFA perfusion and post-fixed for 4 hours on ice. After cryoprotected in 30% (w/v) sucrose for two nights at 4°C, brainstem was immerged into OCT and sectioned at 50 μm using the cryostat for free-floating section staining. Sectioned tissues were blocked with 10% goat serum in PBST (PBS containing 0.1% Triton X-100) for 1 hour and incubated with primary antibodies at 4°C overnight. After washing with PBST, secondary antibodies were applied for 2 hours at room temperature. Fluorescence images were taken using Nikon C2 confocal system. Primary antibodies including: rabbit anti-GFP (Invitrogen, A11122, Lot# 1925070; 1:1000), rabbit anti-c-Fos (Santa Cruz Biotechnology, sc-52, Lot# B0112; 1:1000), mouse anti-NeuN (MilliporeSigma, MAB377, Lot# 3205920; 1:1000), goat anti-WGA (Vector Laboratories, AS-2024, Lot# T1112; 1:1000), guinea pig anti-Synaptophysin 1 (Synaptic System, 101 004; 1:200). Secondary antibodies including: goat anti-rabbit IgG-Alexa Fluor-488 (Invitrogen, A11008, Lot# 1797971; 1:500), goat anti-rabbit IgG-Alexa Fluor-555 (Invitrogen, A21429, Lot# 1683674; 1:500), Goat anti-mouse IgG-Alexa

Fluor-Cyanine5 (Invitrogen, A10524, 1:500), Cy3 AffiniPure Donkey Anti-Goat IgG (Jackson ImmunoResearch, 705165147, Lot# 148575; 1:500), goat anti-guinea pig IgG-Alexa Fluor-555 (Invitrogen, A21435; 1:500).

Neuronal ablation by NMB-saporin

WT mice were anesthetized by ketamine / xylazine and secured in the stereotaxic apparatus (Leica, Model# 39477001). NMB-saporin (Advanced Targeting Systems, Cat. #IT-70; 50 ng in 50 nL) or blank-saporin (Advanced Targeting Systems, Cat. #IT-21; 50 ng in 50 nL) was injected into the spinal trigeminal nucleus region via the coordinates (−7.60 mm posterior to bregma, −6.70 mm ventral from surface, ± 1.50 mm from midline).

Retrograde neuronal tracing from the caudal ventral respiratory group (cVRG)

Alexa 555 conjugated cholera toxin subunit B (CTB-555, Invitrogen, C34776, Lot# 2086750; 100 ng in 50 nL) was injected into the cVRG of *Nmbr*$^{eGFP/+}$ mice. The coordinates were: −5.60 mm posterior to lambda, −1.30 mm ventral from the brainstem surface, ± 1.30 mm from midline. Five to seven days after injection, brainstems were collected for sectioning and immunofluorescence staining.

Brainstem preparation and electrophysiological recordings

Male mice (14-21 days old) were deeply anesthetized with isoflurane and decapitated at the cervical spinal level. The brainstem was removed and placed in ice cold solution containing (in mM): Sucrose 209, KCl 2, NaH_2PO_4 1.25, $MgCl_2$ 5, $CaCl_2$ 0.5, $NaHCO_3$ 26 and glucose 10, saturated with 95% O_2, 5% CO_2. Brainstem was vertically embedded in agar and transverse sliced (350 μm per slice) from caudal to rostral using a Vibratome (Vibratome Series 3000 Plus Tissue Sectioning System). Slices were allowed to recover at 34°C for 30 min in holding artificial cerebrospinal fluid (ACSF) containing (in mM): NaCl 92, KCl 2.5, NaH_2PO_4 1.25, $NaHCO_3$ 30, $MgCl_2$ 2, $CaCl_2$ 2, glucose 25 and HEPES 20, saturated with 95% O_2, 5% CO_2. Slices were placed at room temperature for one hour prior to recording. After incubation, slices were placed in a recording chamber continuously superfused with oxygenated recording ACSF containing (in mM): NaCl 124, KCl 2.5, NaH_2PO_4 1.25, $NaHCO_3$ 24, $MgCl_2$ 1, $CaCl_2$ 2, glucose 12.5 and HEPES 5. Whole-cell current-clamp recordings were performed on cVRG region of brainstem slices using a MultiClamp 700B amplifier and pCLAMP 10.5 software (Molecular Devices). The internal solution contained the following (in mM): K^+-gluconate 130, NaCl 10, $MgCl_2$ 1, EGTA 0.2, HEPES10, Mg-ATP 1, Na-GTP 5 with an osmolarity of 290–300 mOsm and a pH that was adjusted to 7.25 using KOH.

NMB peptide injection into the caudal ventral respiratory group (cVRG)

WT and *Nmbr*$^{-/-}$ mice were anesthetized with 2% isoflurane and secured in the stereotaxic apparatus (Leica, Model# 39477001). NMB peptide (TOCRIS, 1908; 1 pmol in 100 nL) was injected into the cVRG region. The coordinates were: −5.60 mm posterior to lambda, −1.30 mm ventral from the brainstem surface, ± 1.30 mm from midline. Sneezing test was performed 10 min after injection, which allowed recovery from isoflurane anesthesia. Mice were euthanized after test and injection sites were checked to exclude the off-target injections.

QUANTIFICATION AND STATISTICAL ANALYSIS

All data are presented as the mean ± standard error of the mean. Sample sizes were chosen based on the "Sample size determination" (Dell et al., 2002), analysis of relevant prior studies and our pilot studies, and considerations including technical restrains, resource availability, and ethical use. No datapoint or result from a successful experiment was excluded from analysis. Unless otherwise defined n numbers in figure legends represent biological replicates (the number of mice). Statistical significance for the two groups was determined using a two-tailed Student's t test. For three or more groups, statistical significances were tested using a one-way ANOVA followed by Tukey-Kramer post hoc tests. Difference between groups were considered statistically significant if $p \leq 0.05$. All statistical testing were performed using Prism 8 (GraphPad, San Diego, CA).

Supplemental figures

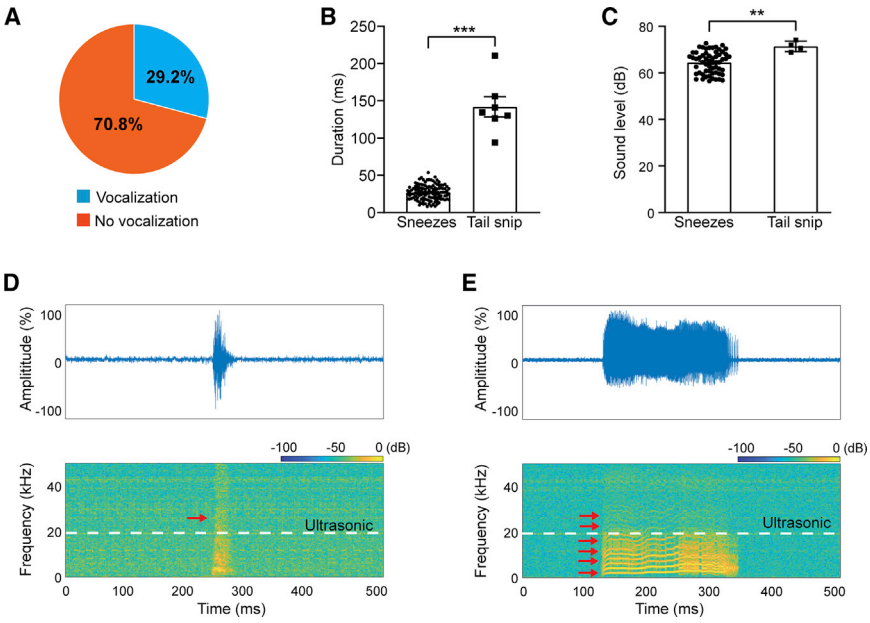

Figure S1. Characterization of sneeze sound in mice, related to Figure 1

(A) Nociception-associated vocalization was observed in 29.2% of mice (7 out of 24 mice) that received a painful tail snip. (B) The duration of sneeze sound (n = 119 sneezes recorded from 11 mice) is significant shorter than nociception-associated vocalization (n = 7 mice). (C) The sound level of mouse sneezes (n = 59 sneezes recorded from 6 mice) is significantly lower than nociception-associated vocalization (n = 4 mice). (D) Representative oscillogram and spectrogram of mouse sneeze sound (indicated by a red arrow). (E) Representative oscillogram and spectrogram of mouse nociception-associated vocalization, which is characterized by broadband consisting of several harmonics (indicated by arrows). Data are represented as mean ± SEM. **$p < 0.01$; ***$p \leq 0.001$

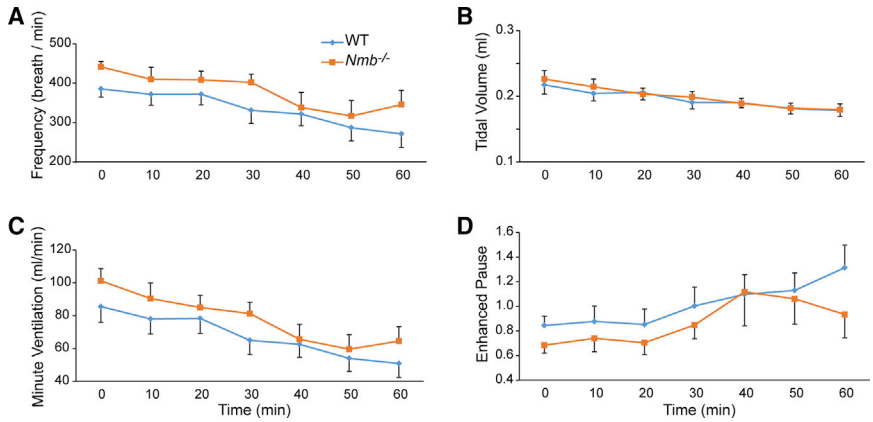

Figure S2. Deficiency in the neuropeptide NMB does not alter eupneic breathing of freely moving mice, related to Figure 3

Whole body plethysmography recording revealed comparable respiratory parameters between WT and *Nmb*$^{-/-}$ mice: (A) respiratory frequency, (B) tidal volume, (C) minute ventilation, and (D) enhanced pause. Due to the prolonged recording period, mice fell asleep and resulted in the gradual decreases in respiratory frequency, tide volume and minute ventilation with time.

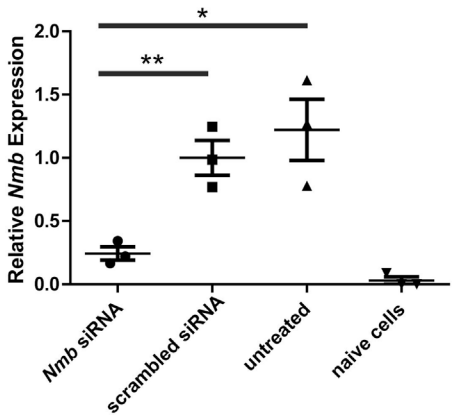

Figure S3. siRNA-mediated knockdown of *Nmb* expression, related to Figure 4

The efficiency of *Nmb* siRNA was tested by co-transfection of HEK293 cells with *Nmb* siRNA and the expression constructs of *Nmb*. Real-time quantitative RT-PCR shows that *Nmb* siRNA efficiently knocked down the expression of *Nmb*, compared with cells co-transfected with *Nmb* expression constructs and scrambled siRNA (scrambled siRNA) or *Nmb* constructs alone (untreated). Naive HEK293 cells, which do not express *Nmb* mRNA, were used as a negative control (naive cells). Three replicates / group; each dot represents one replicate. Data are represented as mean ± SEM. *$p \leq 0.05$, **$p \leq 0.01$.

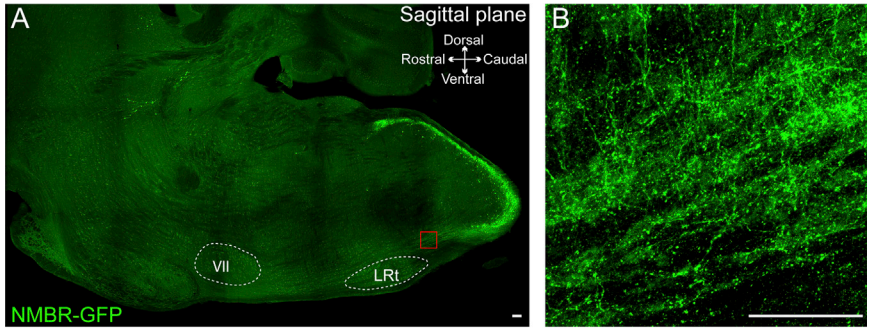

Figure S4. NMBR^{+} neurons selectively project to the caudal ventral respiratory group, related to Figure 6

(A) Representative sagittal image showing that NMBR^{+} neurons selectively project to caudal ventral respiratory group (cVRG) (the region around the red box), as revealed by axonal tracing in *Nmbr*^{eGFP} reporter line. LRt, lateral reticular nucleus; VII, facial motor nucleus. (B) Higher magnification view of the boxed region in (A). Scale bars: 100 μm